# Glacial and Holocene terrestrial temperature variability in subtropical east Australia: branched GDGT distributions in a sediment core from Lake McKenzie

Authors: Woltering M.[1*] †,, Atahan P.[2], Grice K.[1], Heijnis H.[2], Taffs K.[3], Dodson J.[2]

Affiliations:

[1] WA-Organic and Isotope Geochemistry Centre, Department of Chemistry, Curtin University, Perth, WA, Australia

[2] Institute for Environmental Research, Australian Nuclear Science and Technology Organisation, Sydney, PMB 1 Menai NSW 2234, Australia

[3] Southern Cross Geoscience and School of Environment, Science and Engineering, Southern Cross University, PO Box 157, Lismore NSW 2480, Australia

†, current address: CSIRO Earth Science and Resource Engineering, Australian Resources Research Centre, Kensington, Perth WA 6151 Australia

* Corresponding author: *Martijn.Woltering@csiro.au*

Keywords: temperature reconstruction, Australia, subtropical, temperature proxy, branched GDGT, Paleolimnology, Lake, Fraser Island, Holocene, Last Glacial Maximum

**Abstract: Branched glycerol dialkyl glycerol tetraether (GDGT) distributions observed in a sediment core from Lake McKenzie were utilized to quantitatively reconstruct the pattern of mean annual air temperature (MAAT) from coastal subtropical eastern Australia between 37 to 18.3 cal ka BP and 14.0 cal ka BP to present. Both the reconstructed trend and amplitude of MAAT changes from the top of the sediment core were observed to be nearly identical to a local instrumental MAAT record from Fraser Island, providing confidence that in this sediment core branched GDGTs could be used to produce a quantitative record of past MAAT. The reconstructed trend of MAAT during 37 to 18.3 cal ka BP and timing of the Last Glacial Maximum (LGM) in the Lake McKenzie record were in agreement with previously published nearby marine climate records. The amplitude of lower than present MAAT during the LGM potentially provide information on the latitude of separation of the Tasman Front from the East Australian current in the subtropical western Pacific. The Lake McKenzie record shows an earlier onset of near modern day warm temperatures in the early Holocene compared to marine records and the presence of a warmer than present day period during the mid-Holocene.**

## Introduction:

Continental climate dynamics in Australia over the last 35,000 years are poorly understood. This is in part the result of a paucity of long, quantitative and well dated climate reconstructions distributed over this continent (Reeves et al. 2013). Most of the information about the thermal history of Australia comes from sea surface temperature reconstructions from marine archives, from palynological reconstructions studies and from amino acid racemisation studies of emu eggs (Reeves et al. 2013 and reverences therin). Although these methods has provided valuable insights on continental climate in Australia there issues concerning the independence, resolution and quantitative nature of these kind if temperature reconstructions (Kershaw and Nanson, 1993; Miller et al., 1997; Moss and Kershaw, 2000; Pickett et al., 2004; Webb, 1986)

A potential and relatively novel way to obtain prospective independent temperature information from the continents is based on the relative distribution of glycerol dialkyl glycerol tetraether (GDGT) lipids observed in lacustrine sediment archives. Branched GDGTs are a set of core membrane lipids with sn-1, 2 stereochemistry and basic *n*-alkyl

chains, with varying numbers of methyl branches and cyclopentane moieties (Sinninghe Damsté et al., 2000; Weijers et al., 2006). The specific sn-1, 2 stereochemistry these membrane lipids suggests a bacterial origin of these lipids (Weijers et al., 2006), although the specific bacterial source of all of the branched GDGTs is yet to be identified. A relationship of branched GDGT distributions with temperature was first identified in a globally distributed soil sample set studied by Weijers et al. (2007b) and lead to the introduction of the methylation index of branched tetraethers (MBT) and the cyclisation ratio of branched tetraethers (CBT) that together could be used as a proxy to infer past continental temperatures based on the branched GDGT distributions in a given sample. The MBT/CBT index from terrestrial soils has subsequently been used to estimate paleotemperatures in marine sediment cores from coastal regions (Rueda et al., 2009; Weijers et al., 2007a), and potentially be additionally used to reconstruct the paleotemperature from lacustrine sediment cores (e.g. Tierney et al., 2010; Niemann et al., 2012).

Although many studies observed that branched GDGTs are ubiquitously found in lake sediments (e.g. Niemann et al., 2012; Sinninghe Damsté et al., 2009; Tierney et al., 2010; Tyler et al., 2010), numerous studies have found evidence suggesting that branched GDGTs in the many lake sediments were not only derived from the surrounding soils. Instead, at least part of the branched GDGTs appear to have been produced within the water column or sediments of these lakes (Bechtel et al., 2010; Loomis et al., 2011; Sinninghe Damsté et al., 2009; Tierney and Russell, 2009; Tierney et al., 2012). In these lakes with *in situ* branched GDGT production the application of the soil calibration by Weijers et al. (2007a) consitently resulted in weakly correlated, and uniformly lower than instrumental records of water or nearby air temperatures. Regional and global lake calibrations (e.g. Loomis et al. 2012; Pearson et al. 2011 and Sun et al., 2011) are currently available that may be better suited to inferring temperatures from lake sediments where *in situ* production of branched GDGTs is

apparent. Several studies have used branched GDGT distributions in lake sediments to produce temperature reconstructions (Das et al., 2012; Fawcett et al., 2011; Loomis et al., 2012; Niemann et al., 2012; Sinninghe Damsté et al., 2012; Tyler et al., 2010). In some of these studies it was observed that the reconstructed temperature trends (Niemann et al., 2012; Loomis et al.,2012, Das et al. 2013) showed a certain degree of agreement with other paleoenvironmental reconstructions or instrumental temperature records. This demonstrates the potential of using branched GDGTs distributions in lake sediments as a proxy for paleotemperature. However in other studies like Sinninghe Damste et al. (2012) and Tyler et al. (2010) reconstructed temperature trends did not appear to match any proxy or instrumental temperature records indicating the successful application of this proxy is still relatively poorly understood.

Here we report the results of a study that determined branched GDGT distributions in a dated sediment core from Lake McKenzie on Fraser Island in subtropical Eastern Australia. Based on a comparison with a local instrumental temperature record it was assessed if branched GDGT distributions could be used as a paleotemperature proxy and produced a reconstruction of the trend and amplitude of temperature changes in subtropical eastern Australia that covered both the end of the last Glacial and Holocene periods. The produced Lake McKenzie temperature record was subsequently compared to other paleoclimate records and interpreted in a paleoclimate perspective.

## Materials and Methods:

*Site location and sampling description:*

Lake McKenzie is (25°26’51”S, 153°03’12”E, 90m asl) is a perched oligotrophic lake, located on Fraser Island (Fig.1). The lake is ca. 1200 meters long and up to ca. 930 meters wide and has a depth up to 8.5m. Lake McKenzie is lined by an impermeable base of

cemented organic matter (Longmore, 1997). Lake McKenzie was formed when organic matter, such as leaves, bark, and dead plants, gradually build up and hardens a depression created by the wind, creating an impermeable layer. Rainfall accumulated in this depression creating a lake. Lake McKenzie sits above the regional aquifer and does not have an inflow or outflow creek and therefore can be considered to be hydrologically closed basins of rainwater (IUCN, 1992), making the lake level highly susceptible to changes in precipitation and evaporation. The water of Lake McKenzie is acidic, with a pH level of 3.7-4.8 (Hadwen, 2002) due to input from organic acids as a result of decaying organic matter. The soils surrounding Lake McKenzie are rapidly draining aeric podosols that consist of aeolian siliceous sands that show low soil development and low nutrient availability (McKenzie et al., 2004).

Two adjacent sediment cores were extracted from the centre of the deepest basin of Lake McKenzie in 2010, in ca. 8.3 m water depth. The cores (LM1 and LM2) were extracted using a gravity corer, extruded on the lake edge, and sliced into either 0.25 cm thick (LM1) or 1 cm thick (LM2) samples. Total un-extruded core length was measured at regular intervals during sampling to monitor loss of core length. Samples were placed in individual plastic zip-lock bags before being transported and stored in laboratory freezers.

In addition to sampling of a sediment core from Lake McKenzie, soil samples (top 10 cm) were collected from 3 locations in the drainage basin (Fig.1) in May 2012. These samples were stored in zip-lock bags for transport and storage in a laboratory freezer before extraction and analyses.

*Age model based on $^{210}Pb$ and $^{14}C$ AMS dates:*

The age model of core LM2 is based on twelve $^{14}C$ AMS and five $^{210}Pb$ ages. With the exception of one large wood fragment recovered from core LM1, terrestrial plant

123 macrofossils, such as leaves or seeds, were not encountered in either sediment cores. For this
124 reason pollen concentrates were prepared for AMS $^{14}C$ dating. Physical and chemical pre-
125 treatment of Lake McKenzie samples was conducted prior to AMS $^{14}C$ measurement with the
126 purpose of isolating pollen and removing contaminants. Samples were sieved to collect a 10-
127 150 μm size fraction, separated by heavy liquid flotation (LST; SG = 1.8) and treated with
128 NaOH (10%), HCl (10%) and $H_2SO_4$ (98%). Pre-treatment of the wood fragment followed
129 the standard acid-alkali-acid method used at the Australian Nuclear Science and Technology
130 Organisation (ANSTO) (Hua et al., 2004). Radiocarbon dates were calibrated using the
131 INTCAL 09 calibration curve (Reimer et al., 2009). Calibrated ages in the paper are reported
132 relatively to present (1950 CE) and are followed by a 'cal ka BP' post-fix. Single dates
133 mentioned in the paper refer to the median age in the 2σ calibrated age-range.

134 Abundance of atmosphere-derived $^{210}Pb$ ($^{210}Pb_{unsupported}$) in the upper sediment was used to
135 estimate recent sediment accumulation rates at Lake McKenzie. The method, which has been
136 described in detail by Appleby and Oldfield (1978), Appleby and Oldfield (1992) and
137 Appleby (2001) uses down-core change in $^{210}Pb_{unsupported}$ activity to calculate an accumulation
138 rate based on the $^{210}Pb$ half-life of 22.26 ±0.22 years. $^{210}Pb_{unsupported}$ was estimated by
139 subtracting activity of supported $^{210}Pb$ ($^{210}Pb_{supported}$), derived from in situ decay of Radium-
140 226 ($^{226}Ra$), from total $^{210}Pb$ ($^{210}Pb_{total}$) activity, which was measured indirectly from its
141 progeny polonium-210 ($^{210}Po$). $^{210}Pb_{supported}$ was measured indirectly from its grandparent
142 radioisotope $^{226}Ra$. Both the CIC (constant initial concentration) and the CRS (constant rate
143 of supply) models (Appleby and Oldfield, 1978; Appleby, 2001) were used to calculate
144 calendar ages.

145 $^{210}Pb_{supported}$ and $^{210}Pb_{total}$ were measured in the upper 8.5 cm of core LM1. Between 0.18 and
146 1.23 g of sediment was prepared by heating the samples in $HNO_3$ at 60°C. Once evaporated,
147 small amounts of $H_2O_2$ (10%) were added with heating until the reaction subsided. The

148 samples were evaporated again before refluxing in a mixture of $HNO_3$ and HCl (1:3; 50-
149 60°C) for at least 4 hours. Samples were subsequently redissolved in HCl (6M) and
150 centrifuged to separate the supernatant from the residue. The residue was washed and
151 discarded. The supernatant and the residue wash were collected and processed to remove
152 excess iron by diethyl ether solvent extraction. The recovery of the preparation method was
153 assessed using radioactive tracers $^{133}$Ba (~85 Bq) for $^{226}$Ra recovery and $^{209}$Po (~0.2 Bq) for
154 $^{210}$Po recovery, which were added at the start of the sample processing procedure. $^{210}$Po and
155 $^{209}$Po were isolated by auto-deposition onto silver discs using $NH_2OH.HCl$, and then analysed
156 with ORTEC alpha spectrometers. $^{226}$Ra and $^{133}$Ba were isolated by co-precipitation and
157 collected as colloidal micro-precipitates on 0.1 μm Millipore VV membrane filters. $^{133}$Ba was
158 analysed using a HPGE gamma spectrometer and $^{226}$Ra was analysed using ORTEC alpha
159 spectrometers.

160 *Total organic carbon (%TOC):*

161 All samples from core LM1 and LM2 were treated with HCl (10%) to remove
162 carbonates before analysed on a Flash 2000 HT Elemental Analyser for TOC%.

163 *GDGT lipid extraction and analysis:*

164 All sediment and soil samples were freeze dried before extraction commenced. About
165 1–5 g of sediment and ~35 grams of soil sample was extracted using a Dionex accelerated
166 solvent extractor (ASE) 200 system using a 9:1 v:v dichloromethane (DCM): methanol
167 (MeOH) mixture. Total lipid extracts were separated into non-polar and polar fractions over a
168 small $Al_2O_3$ column in a pasteur pipette, using hexane: DCM (9:1, v:v) and DCM: MeOH
169 (1:1, v:v) as eluents (Schouten et al., 2007). The polar fraction containing the GDGTs was
170 dried, redissolved in hexane: isopropanol (99:1, v:v) and filtered with a 0.45 μm filter. High
171 performance liquid chromatography–atmospheric pressure chemical ionization–mass

spectrometry (HPLC–APCI–MS) analysis was carried out on a Thermo Oribtrap XL LC/MSD using scan window of (1015-1305 *m/z*). For data analysis different 0.1 amu scan windows were created for crenarchaeol (IV, *m/z* 1292.2), and the nine different branched GDGTs (III, *m/z* 1050; IIIb, *m/z* 1048; IIIc, *m/z* 1046; II, *m/z* 1036; IIb, *m/z* 1034; IIc, *m/z* 1032; I, *m/z* 1022; Ib, *m/z* 1020; Ic, *m/z* 1018 (Weijers et al., 2007b). Peak areas were integrated following the methods described in Weijers et al. (2007b). Each sample was measured at least three times or more, and measured over multiple days, to determine the analytical error associated with the precision and reproducibility of these analyses. The standard deviation was calculated for each sample and is plotted in figures with the 2σ (95%) confidence interval of the results.

**Results and discussion:**

*Age model for core LM2 from Lake McKenzie*

The obtained $^{14}$C AMS and $^{210}$Pb dates from cores LM1 and LM2 are shown in Table 1 and 2. A common depth axis for the adjacent cores was constructed using linear interpolation between tie-points identified on the %TOC curves (Fig.2). A deposition model was constructed using the OxCal (v4.1) P_Sequence model ($k$ = 4) (Bronk Ramsey, 2009). Three of the AMS $^{14}$C dates were identified as being outliers (OZ0411, OZN680 and OZN681), and were excluded from deposition model calculations. The exclusion of these dates as outliers was based on: their poor fit with other radiocarbon dates based on linear regression, the lower overall Agreement Index produced when suspected outlying dates were included individually in P_Sequence deposition models, and the results of OxCal outlier analyses showing the dates as having higher posterior probabilities of being outliers compared with the other dates. The reason for these $^{14}$C AMS dates yielding younger ages compared to the other samples is not currently known. Potentially the $^{14}$C dates from pollen extracts may be affected by terrestrial

196 reworking, which could result in these samples have older $^{14}C$ ages than the material
197 produced within Lake McKenzie. Unfortunately, organic matter from core LM2 was not $^{14}C$
198 dated which potentially could have shed light on the potential reworking of terrestrial pollen.
199 A large observed difference in the age of pollen from 26 and 27 cm depths indicates almost
200 no sedimentation occurred between ~14.0±0.7 and 18.3 ±0.5 cal ka BP (Fig.3A) and
201 therefore could be represent a hiatus in sedimentation when Lake McKenzie may have dried
202 up or was ephemeral.

203 According to the $^{210}Pb$ and $^{14}C$ age models Lake McKenzie has experienced a wide range of
204 sedimentation rates in the past: ~160 year/cm at the bottom, ~900 years/cm in the LGM
205 section of the, ~660 years /cm after the hiatus in sedimentation and ~18 years/cm in 210Pb
206 dated top section of core LM2. The low sedimentation sedimentation rates in the $^{14}C$ dated
207 sections of LM2 are in the range of other lakes on Fraser Island like Lake Coomboo
208 Depression (~1000 years/cm, Longmore and Heijnis, 1999) and Lake Allom (~ 133 years/cm,
209 Donders et al., 2006). These low sedimentation rates are not unexpected as Fraser Island is
210 sand island dominated by rainforest vegetation, where sediment sources are few (Donders et
211 al., 2006). That overall Lake Allom exhibits higher sedimentation rates than Lake McKenzie
212 can be explained differences in physical and chemical characteristics: Lake McKenzie has
213 markedly clearer water, lower Total Phosphorus, Total Nitrogen and Ch-a content compared
214 to Lake Allom (Bowling, 1988; Hadwen et al., 2003; Longmore, 1998). Whether these
215 parameters are related to a low rate of productivity or high rate of sediment diagenesis, and
216 thus a slow sediment accumulation rate at Lake McKenzie, remains to be tested
217

218 The sediment accumulation rate calculated from $^{210}Pb_{unsupported}$ activity is much higher than
219 that estimated for the underlying sediments dated using radiocarbon. The high water content,
220 and low bulk density (Hembrow et al., 2013), of the upper layers of sediment may account in

part for this shift in sediment accumulation rate at 7 cm depth. Higher densities and lower water content were observed $^{14}C$ dated sections of core LM2 densities observed in the 30-24 cal ka BP period (Hembrow et al., 2013) suggesting that sediment compaction is a factor cin LM2.Additionally there may have been a reservoir age affecting the $^{14}C$ dates, which were based on pollen extracts, or a difference in the transport rates of the two types of material dated (fine grained organic material compared to $^{210}Pb$ carrying particles). Bioturbation does not appear to have played a major role at core LM2 in recent years as a clear monotonic decrease in $^{210}Pb_{unsupported}$ with depth is observed in the upper part of the record.

With the current information however it is imposable to further evaluate the robustness of the age model for core LM2. However the timing of the LGM and a mid-Holocene temperature optimum in core LM2 (discussed below) agrees with marine record and therefore may be an indication that the age model for LM2 is not seriously biased.

*Branched GDGT distributions as a potential paleotemperature proxy for core LM2 and a strong observed agreement with the instrumental record:*

GDGT distributions in core LM2 were dominated by branched GDGT lipids, with isoprenoid GDGT lipids making up less than 5%.Branched GDGT distributions were dominated by branched GDGT 1 (*m/z* 1022), that contributed ~ 75% of all branched GDGT lipids.

A range of different soil (Peterse et al., 2012; Weijers et al., 2007b) and lake (Loomis et al., 2012; Pearson et al., 2011; Sun et al., 2011; Tierney et al., 2010; Zink et al., 2010) branched GDGT calibrations have been published that could be used to calculate temperatures. Loomis et al. (2012) use different branched GDGT ratios to calculate temperatures based on1: the MBT/CBT ratio, 2: the main Branched GDGTs (MBR) or 3: a selection of branched GDGTs

245 based on selective forward selection (SFS). Sun et al. (2011) calibrated both against MAAT
246 or the temperature of the warm season (Tw). All calibrations were evaluated to determine
247 whether the choice of calibration significantly affected the resulting paleotemperature
248 reconstruction for Lake McKenzie (Fig.4).

249 The selection of calibration was observed to have a have a significant effect on the
250 resulting paleotemperature reconstructions (Fig.4), although all calibrations indicated that
251 MAAT was significantly lower during the end of the last glacial period compared to the
252 Holocene. Large disagreements were observed among the reconstructions among the pattern
253 and amplitude of past reconstructed temperature changes, as well in the absolute values of the
254 inferred temperatures (Fig.4). The MAAT reconstruction using the soil calibrations (Peterse
255 et al., 2012; Weijers et al., 2007b) and the MAAT and Tw calibrations of Sun et al. (2011)
256 showed good agreement in the pattern of reconstructed MAAT, but differed in estimates of
257 amplitude of past MAAT changes and the absolute values of infered temperatures(Fig.4).
258 Similary the Loomis et al. (2012 MBR) and Zink et al. (2010) MBT reconstructions agreed in
259 the trend of reconstructed MAAT, but differed in amplitude of MAAY changes and the
260 values of inferred MAAT(Fig.4). All other calibrations (Pearson et al., 2011, Tierney et al.,
261 2010, Loomis et al. 2012 SFS and MBT) resulted in unique patterns of reconstructed MAAT
262 variability within core LM2 (Fig.4). The coice of calibration does affect the produced record
263 of inferred temperatures from core LM2. Therefore it was important to determine which
264 calibration provides the most accurate estimates of past temperature.

265 According to the $^{210}$Pb age model, the top 1 cm slice of sediment from core LM2
266 covers a period of sediment accumulation of between 1991 and 2005. Inferred MAAT values
267 from this sediment based on the different calibration ranged from 18.1-40.7$^{o}$C (Fig.4, Table
268 3). Comparison of these estimates with an instrumental record may provide information about
269 the performance of the different calibrations. The weather station located on the mainland at

Maryborough (Fig.1, of BOM weather station: 040126) is the nearest weather station that contained a complete record between 1991-2005. In overlapping years this weather station was in agreement with a nearer, but incomplete record of MAAT from Eurong (BOM weather station: 0040478) located near Lake McKenzie. Therefore absolute MAAT measured at Maryborough was assumed to be similar than what Lake McKenzie experienced. Most calibrations yielded estimates of MAAT for the top 1cm sediment that were significantly higher than the instrumentally measured MAAT at Maryborough (21.5$^{o}$C). The Pearson et al. (2010) or the Sun et al. (2012 Tw) calibrations were calibrated using warm season/summer temperatures and thus cannot be compared to instrumentally measured MAAT. Both soil calibrations of Weijers et al. (2007b) and Peterse et al. (2012) yielded MAAT estimates (25.4 and 20.4$^{o}$C) that were considering calibration errors (4.8 and 5.0$^{o}$C) in agreement with instrumentally measured MAAT. None of the lake MAAT calibrations produced MAAT values that were near the instrumentally measured MAAT and with exception of the Tierney et al. (2010) calibration, all significantly overestimated inferred MAAT. With the limited information about the branched GDGT producers it would be speculative to assume branched GDGTs in core LM2 would reflect a MAAT and not a seasonal temperature. Therefore the above observations are not sufficient to determine that soil calibrations were most applicable for inferring MAAT from core LM2.

Instead the performances of each calibration were evaluated according to how accurately the trend and amplitude of past MAAT variability was reconstructed relative to a local instrumental temperature record. The top five sediment slices from core LM2 cover 95 years of sediment accumulation (from 1910-2005), according to the $^{210}$Pb age model. This therefore overlaps with local instrumental MAAT records. The above discussed weather station at Maryborough was not used for this comparison as the long term temperature record from this station was classified as potentially being affected by increased urban development

295 in the late 20th century (BOM, 2013). This resulted that this station recorded a higher
296 temperature increase (1.7°C) during the investigated period compared to other proximal
297 weather stations (1.0°C). Instead the MAAT record from Sandy Cape Lighthouse (BOM
298 weather station: 039085) was used for evaluating the performance of the different
299 calibrations. This weather station is located within a preservation area on Fraser Island,
300 approximately 60km north of Lake McKenzie (Fig.1). At this weather station MAAT
301 increased by approximately 1.0°C between 1910-2005 and both the amplitude and pattern of
302 change were nearly identical to those observed in other regional and state wide climate
303 temperature records (BOM, 2013). For overlapping years the Sandy Cape Lighthouse
304 recorded approximately 1.2°C higher temperatures compared to the weather stations at
305 Eurong and Maryborough. This higher temperature may be may be in part explained by the
306 lower latitude of the Sandy Cape Lighthouse compared to Eurong and Lake McKenzie.
307 Additionally the location of Sandy Cape Lighthouse may reflect more marine like climate
308 compared to Eurong and Maryborough which may explain the average higher tempted at this
309 station. Besides this systematic offset in MAAT, both the pattern and amplitude of changes in
310 MAAT observed between 1910 and 2005 are assumed have been similar at both Sandy Cape
311 Lighthouse and Lake McKenzie.

312 All of the branched GDGT calibration produced temperature reconstructions that were
313 significantly correlated ($P<0.05$) with the instrumental record of average MAAT. The
314 observed correlation coefficients of these comparisons ranged between 0.618-0.961 and the
315 six most strongly correlated ($R^2$= 0.929-0.961) cross-plots are shown in Fig. 5. Of the fix
316 most strongly correlated calibrations five used CBT/MBT ratios to infer temperature from
317 branched GDGT distributions. These high correlation coefficients suggest that those
318 calibrations accurately captured the trend of MAAT changes. Besides reconstructing the
319 trend, the best calibration should also be able to quantitatively reconstruct the amplitude of

MAAT changes. This can be evaluated by comparing the slope value of the relationship between instrumental and reconstructed MAAT, where the most accurate calibration would have a value near 1. The soil calibration of Peterse et al. (2012) produced a value for the slope that was very close to one, while all other highly correlated calibrations produced slope values that were significantly higher than one (Fig.5). These higher slope values indicate that these calibrations may substantially overestimate the reconstructed amplitude of MAAT changes. The soil calibration of of Peterse et al. (2012) accurately captured both the trend and amplitude of observed MAAT changes during the studied period and therefore seems the calibration of choice for quantitatively inferring temperatures from core LM2. To our knowledge, this is the first time such good agreement has been observed between an instrumental temperature record and branched GDGT temperature reconstruction from a lacustrine sediment core providing confidence in the qualitative quality of the produced MAAT record.

This good agreement between branched GDGT inferred and instrumental temperatures can be in LM2 may be seen as remarkable considering the large calibration error of the Peterse et al. 2012 calibration and the observed analytical error ($< \pm 0.4^{o}C$). However when comparing temperature estimates form single sediment core the overall uncertainty caused by the calibration error may be significantly smaller than $5^{o}C$. The large scatter of the Peterse et al. (2012) calibration is likely reflecting that besides pH and temperature potential other environmental, geological or biological factors may affect branched GDGT distributions in the global soil dataset that are not accounted for. It is much more likely that the unincorporated factor can vary much greater within a global dataset compared to branched GDGT distributions from a single location or sediment record (Peterse et al. 2011). The actual influence of the calibration error on the reconstructed trend and amplitude of the MAAT reconstruction from this single sediment core may be considered to

345 be relativly small or systematic of nature. Although a local calibration would be required to
346 determine the actual uncertainty in the inferred temperature estimates from core LM2, the
347 nearly identical pattern of inferred and instrumentally measured MAAT does not suggest that
348 the large calibration error of the Peterse et al. (2012) calibration had a significant effect on
349 the accuricy of the reconstructed pattern and amplitude of MAAT changes. Additionally the
350 good agreement between instrumental and inerred MAAT in LM2 shows that by measuring
351 each samples at least in triplicate, and comparing mean temperature estimates, relativly small
352 temperature changes (<1$^{o}$C) appear to be accurately reconstructed.

353 *An allochthonous origin of branched GDGTs in the sediment of Lake McKenzie*

354 That the calibration of Peterse et al. (2012) accurately reconstructed both the trend
355 and amplitude of past MAAT variability, suggests an allochthonous and probably soil derived
356 origin of the branched GDGTs observed in the Lake McKenzie sediments. A comparison
357 between the environmental parameters and branched GDGT distributions observed in soils
358 and the lake sediment could provide evidence for this.

359 There is a significant difference in the pH of the water column of Lake McKenzie and
360 the soils surrounding the lake: the soils surrounding Lake McKenzie consist of rapidly
361 draining aeric podosols that are only slightly acidic (pH =5.8, McKenzie et al., 2004),
362 whereas the water column of Lake McKenzie is acidic over the entire annual cycle (pH 3.7-
363 4.8, Hadwen, 2002). This difference in pH combined with the sensitivity of branched GDGT
364 distributions to pH, provides an opportunity to compare branched GDGT distributions
365 measured in soils and the lake sediment to determine whether the branched GDGTs observed
366 in the sediment of Lake Mckenzie are of predominatly alochthonous or autochthonous origin.

367 The branched GDGT distributions determined in three soil samples (top 10cm)
368 surrounding Lake McKenzie were observed to be nearly identical to those observed in the top

1cm sediment slice of core LM2 in Lake McKenzie (Fig.6A). In both the soils and in the top sediment slice, branched GDGT distributions are dominated by branched GDGT 1 (*m/z* 1022) which is a feature more commonly observed in soil samples, rather than lake sediments that may contain branched GDGTs produced *in situ* (Fig.6B). These observations are consistent with a predominantly allochthonous origin for the branched GDGTs observed in Lake McKenzie.

Further potential evidence of a predominantly allochthonous origin of branched GDGTs in Lake McKenzie was observed from the CBT reconstructed pH values from both the sediment slice and the soil samples (Fig.7) . Depending on which CBT calibration was applied, pH estimates from the top sediment slice ranged from 5.9 (Peterse et al., 2012), to 6.1 (Weijers et al. 2007b) and to 7.1 (Sun et al. 2011). These pH estimates were all significantly higher (higher than the calibration errors of the pH estimates based on branched GDGTs) than the pH of the water column of Lake McKenzie. Instead the reconstructed pH value of Lake McKenzie sediment was nearly identical to both the pH estimate and published pH for the soils surrounding Lake McKenzie (Fig.7). This and the information discussed above, suggests that *in situ* production of branched GDGTs in Lake McKenzie is either minor or non-existent, and this supports the application of the Peterse et al. (2012) soil calibration to infer temperatures and pH values from the branched GDGTs observed in core LM2 from Lake McKenzie.

*Independence of the LM2 temperature reconstruction*

There appears to be some degree of synergy among the reconstructed MAAT, pH and %TOC values determined in core LM2 (Fig.8A). Both inferred MAAT and pH estimates from LM2 indicated higher temperatures and pH values in the Holocene section compared to the end of the Last glacial section of the record. Whereas, %TOC of the sediments was

observed to be significantly lower in the Holocene and high during the end of the Last Glacial sections of the record from LM2. Tyler et al. (2010) previously observed a strong correlation between the CBT and MBT ratios in Lochnagar suggesting that there changes in reconstructed pH values controlled the trend of the reconstructed temperatures. No correlation between the CBT and MBT ratios was observed in the LM2 record (Fig.8B). Both pH and temperature was reconstructed to be low during the end of the last Glacial and higher during the Holocene periods and there appears to be a significant degree of correlation ($R^2$=0.872) between these parameters when the entire record is compared, however the strength of this correlation is reduced to insignificant values (0.373 and 0.183) when pH and MAAT are compared separately for the end of the last Glacial and Holocene periods (Fig.8C). The observed independence of the MBT from the CBT ratio and the lack of correlation between trends of temperatures and pH during the end of the last Glacial and the Holocene periods suggests that the reconstructed trend of MAAT variability was not controlled by changes in pH. Similarly, the relationship between % TOC and reconstructed MAAT appeared to be significantly inversely correlated ($R^2$ =0.658) when values from the entire record were assessed, but the correlation is observed to be either insignificant ($R^2$= 0.258) at the end of the last Glacial or significant ($R^2$=0.673) during the Holocene, but in an opposite direction to the relationship observed over the entire record (Fig.8D). Based on the limited information obtained in this study, no clear evidence indicated that the apparent MAAT reconstruction from Lake McKenzie was controlled by any environmental parameters other than temperature, and therefore the MAAT reconstruction was interpreted as reflecting an independent MAAT record.

*Trend and amplitude of MAAT changes as reconstructed from core LM2*

Due to low sedimentation rates, the 46cm long LM2 sediment core provided information about trend of MAAT variability at subtropical eastern Australia going as far back as 37 cal

418 ka BP. The resolution of the LM2 MAAT record is relatively low due to the slow
419 sedimentation rates and the 1cm thick sample slices. Still, the LM2 record provides
420 information about at least millennium scale MAAT variability at coastal subtropical eastern
421 Australia during Marine Isotope Stage 3 (M.I.S. 3), the Last Glacial, and the Holocene
422 periods. An apparent hiatus in sedimentation between 18.3-14.0 Cal ka BP resulted in the
423 LM2 record not providing information about the trend of MAAT during a large portion of the
424 Last Glacial termination. As discussed above the good agreement with the instrumental and
425 LM2 record indicates that the LM2 MAAT reconstruction potentially provides quantitative
426 estimates of the amplitude of MAAT variability. However, a lack of other quantitative
427 temperature reconstructions from coastal subtropical eastern Australia made it impossible to
428 validate the apparent quantitative nature of the reconstructed trend and amplitude of MAAT
429 variability at Lake McKenzie prior to 1910, when standardized temperature measurements
430 began at weather stations in Australia (BOM, 2013). Instead the produced Lake McKenzie
431 MAAT record was compared to other climate records from within the Australian region and
432 discussed in a paleoclimate perspective for the different climate periods.

433 37-30 ka Late Marine Isotope Stage 3

434 Between 37.3±0.4 and 31.6±0.7 cal ka BP, reconstructed temperatures in the LM2 record
435 were relatively stable and substantially warmer than between 30.2±0.6 and 18.8±0.5 cal ka
436 BP (Fig.9). All MAAT estimates between 37 and 32 ka were observed to be statistically
437 similar and therefore did not suggest significant millennium scale temperature variability. Ice
438 core records from Antarctica do show millennium scale temperature variability through this
439 period with temperature changes up to 2 $^{o}$C (EPICA, 2006). Perturbations in temperature
440 were also observed in the Murray Canyons, offshore from Southern Australia (DeDecker et
441 al. 2012) and in deep oceanic cores from the Southern ocean (Barrows et al. 2007, Armand
442 and Leventer 2010). A lack of perturbations in the LM2 MAAT record suggests that

443 subtropical eastern Australia did not experience a similar change in temperature through this
444 period, although the resolution was not high through this period. This would be in agreement
445 with other low latitude continental records from the southern hemisphere (Tierney et al.,
446 2008; Woltering et al., 2011).

447 30-22 ka early last glacial period

448 Between ~30.2±0.6 and 28.9±0.7 cal ka BP, temperatures in the LM2 record dropped by
449 ~1$^{o}$C relative to the period between 37.3±0.4 and 31.6±0.7 cal ka BP (Fig. 9). The timing of
450 this agrees with studies from Antarctica (Blunier and Brook, 2001), Chile (Denton et al.,
451 1999) and New Zealand (Hellstrom et al., 1998; Vandergoes et al., 2005), that all document
452 cooling at ~30 ka BP, potentially as a result of an insolation minimum in the Southern
453 Hemisphere (Vandergoes et al., 2005). However *G. ruber* $^{18}$O record from core GC-12
454 located approximately 220 km north of Lake McKenzie, did not show a similar decrease of
455 temperature around 30 cal ka BP (Bostock et al. 2006, Fig.10). This difference between
456 proximate temperature records may be due to that LM2 reconstruction being land derived,
457 and therefore more sensitive to changes in radiative forcing relative to the ocean. MAAT
458 increased by approximately 0.5$^{o}$C compared to 30.2±0.6 and 28.9±0.7 cal ka BP, after which
459 the trend in MAAT values showed a general decline in temperatures in toward the LGM (Fig.
460 9). This cooling trend appeared to have started at approximately 27 cal ka BP in the LM2
461 record. This general trend can be also seen in GC-12 marine $\delta^{18}$O record (Bostock et al.
462 2006, Fig.10). A short period of warming and drying in the early glacial period between 26-
463 24 ka was seen in paleoclimate reconstructions from the Australian region (Moss and
464 Kershaw, 2007, Bowler et al. 2012, Calvo et al., 2007; Armand and Leventer 2010). This
465 Coincided with the Kawakawa tephra and the first interstadial of the Last Glacial period in
466 New Zealand (Barrel et al. 2013). A warming period was not observed in the LM2 record
467 during this time period, although this short temperature anomaly could be missed due to poor

chronological control and resolution combined with the uncertainty of the MAAT estimates. At Lake Allom, on Fraser Island to the north of Lake McKenzie, a hiatus is sedimentation was observed between 28- 10 cal ka BP suggesting that during this entire period conditions on Fraser Island were relatively dry (Donders et al., 2006).

22-18 ka Last Glacial Maximum

The LGM globally considered to have occurred between 27-19 Ka BP (Clark et al. 2009). For Australia the timing of the LGM was defined to have started later, it centred on ~21 ka (Suggate, 1990) and lasted 3-4 ka (Barrows et al., 2001; Bowler, 1976; Harrison, 1993), or occurred from 23-18 cal ka BP (D'Costa et al., 1989; Kershaw, 1986; Turney et al., 2006) and was characterized by limited glacial advances in the Snowy Mountans and Tasmanian Highlands. Both of these regions recorded a maximum glacier extent at ~19 ka. The lowest temperature estimate observed in the LM2 MAAT occurs at 18.8±0.5 cal ka BP, ~ 4.1$^{o}$C lower than modern day temperature (Fig.9). This was immediately followed by a hiatus in sedimentation between 18.3-14.0 cal ka BP. The timing of the lowest temperatures during the LGM ~19 cal ka BP in the Lake McKenzie record is in good agreement with a $\delta^{18}O$ *G. ruber* records from north (GC-12) and south (GC-25) of Fraser Island (Bostock et al. 2006; Troedson and Davies, 2001) (Fig. 10). This estimate of the maximum temperature anomaly of the LGM observed in core LM2 is slightly larger than a previously published foraminifera assembly study that estimates a 1-3$^{o}$C anomaly for the subtropical west Pacific Ocean (Barrows and Juggins, 2005). $\delta^{18}O$ values in core GC-12 recorded a 2-3$^{o}$C lower temperatures, while GC-25 yielded $\delta^{18}O$ values that indicated temperatures were 6 $^{o}$C colder (Troedson and Davies, 2001). Bostock et al. (2005) intepreted this difference of temperature amplitude of the LGM between cores GC-12 and GC-25 to reflect a northwards shift in the separation of the Tansman Front from the EAC during the LGM, resulting in warm waters from the EAC not reaching GC-25. The ~4.1$^{o}$C lower MAAT during the LGM

observed in the LM2 reconstruction lies between the reconstructed amplitudes of cores GC-12 and GC-25 which may indicate that the separation of the EAC and the Tasman Front may have occurred more northerly than Lake McKenzie (25°26'S).Althernativly the intermediate LGM anoloaly in the LM2 record may be explained by the effects of lowered sea level at the end of the LGM that resulted in an increased distance between Lake McKenzie and the west Pacific Ocean of approximately 60km. This may have reduced the influence of the EAC on the climate of Lake McKenzie leading to more cooling at Lake McKenzie compared to sites more northerly in the subtropical west Pacific Ocean .

13.3-12.0 ka end of last glacial termination period

Inferred temperatures are highest in the entire record just after the restart of sedimentation ~14 ka BP. (Fig.9). The inferred temperature of ~ 21.5°C at 13.3±0.7 cal ka BP was approximately 1.1°C higher than modern day MAAT. This may potentially indicate that relatively warm conditions occurred on Fraser Island during the Antarctic Cold Reversal or during the early Younger Dryas. A similar high temperature at this time was not observed in nearby $\delta^{18}O$ records from cores GC-12 (Bostock et al. 2006) and GC-25 (Troedson and Davies, 2001) (Fig.10) or other records from the Australia region. Unless the temperatures at Fraser Island were totally decoupled from nearby locations, it seems unlikely that that the peak in MAAT observed in Lake McKenzie record at 13.3±0.7 cal ka BP only occurred that this location. It is not possible to exclude the possibility that this high temperature may be result of a change in source location or seasonality of branched GDGTs produced during and immediately following the hiatus period.

12-8 ka Early to mid Holocene

In the early Holocene between 12.0± 0.6 and 8.1 ±0.7 cal ka BP, temperatures were observed to be near present day temperatures in the LM2 record (Fig. 9). This onset of modern day temperatures early in the Holocene is observed in other paleotemperature proxy records in the Southern Hemisphere (Shakun et al., 2012) and in the central Indo Pacific Warm Pool (IPWP) (Gagan et al., 2004). In comparison, SST in the tropical and temperate regions of Australia moved towards modern day temperatures between ~11-9 ka BP (Petherick et al. 2013, Reeves et al., 2013). Compared to the nearby temperature records GC-12 GC-25 marine $^{18}O$ the LM2 reconstruction reached near modern day temperatures earlier than the surrounding oceans, which showed modern day conditions established at approximately 9ka BP (Bostock et al. 2006; Troedson and Davies, 2001)(Fig. 10). An earlier onset of modern day temperatures of Fraser Island compared to surrounding oceans may be related to the higher sensitivity of terrestrial environments to changes in insulation compared to the delayed response of the oceans due to the higher heat content of the oceans relative to the atmosphere. The observations from the LM2 temperature record together with pollen evidence from Lake Allom on Fraser Island (Donders et al., 2006) suggests that the early Holocene was a period of relatively warm and dry conditions of Fraser Island.

8-5 ka mid Holocene

The mid Holocene period in the Australasian region represents a period when maximum temperatures are observed in terrestrial records, although the highest temperatures appear to occur at slightly different times in different regions (Reeves et al. 2013). Antarctic temperatures stabilized during this period (EPICA, 2004) and in the North the thermal maximum of the IPWP occurred by 6.8-5.5 cal Ka BP (Abram, et al. 2009). During the mid-Holocene (7.1±0.4 and 5.8 ±0.3 cal ka BP) observed temperatures in the LM2 record were higher than the present (Fig.9). The highest temperature was observed 5.8±0.3 cal ka BP and

542 was approximately 0.9°C higher than present day MAAT. This period corresponded with the
543 timing of a thermal optimum of the IPWP (Abram, et al. 2009), although chronological
544 control of the LM2 record is low.The timing of this mid Holocene temperature maximum
545 corresponded with a hiatus in the Lake Allom sediment record between 6.5–5.4 cal ka BP
546 (Donders et al., 2006), suggesting that the period of elevated temperature detected at Lake
547 McKenzie was likely a period of reduced effective precipitation on Fraser Island.
548 Interestingly, the GC-12 and GC-25 δ18O marine records from north and south of Fraser
549 Island did not exibit a mid Holocene temperature optimum (Bostock et al. 2006; Troedson
550 and Davies, 2001) (Fig.10). An almost identical temperature anomaly of 1°C for the mid-
551 Holocene temperature maximum as seen for LM2 has been previously reported for the central
552 Great Barrier Reef, based on Sr/Ca ratios in corals from Orpheus Island (Gagan et al., 1998),
553 although some questions about both the chronology of this coral record (Gagan et al., 1998)
554 and the LM2 record remain**.**

555

556 5-0 ka Late Holocene

557 After the mid-Holocene, temperatures were lower, with values that were near or below
558 present day MAAT between 5.2±0.3 and 2.9±0.2 cal ka BP. Directly after the mid Holocene
559 thermal optimum, MAAT showed a large fluctuation where the MAAT dropped by 1.8°C
560 over a period of approximately 1.8 ka followed by a warming of ~1.2°C over 0.7 ka (Fig.9).
561 At around the same time a high resolution deep sea $\delta^{18}O$ record of *G. bulloides* from South
562 Australia showed several ~1500 year cycles (Calvo et al. 2007). Unfortunately the resolution
563 and chronological control of the LM2 record was not sufficient to determine if the observed
564 fluctuations in this MAAT record showed a similar cyclicity. The LM2 MAAT record during
565 the late Holocene shows a different trend compared cores GC-12 and GC-25 that showed

general increase in temperature during this same period (Fig.10). Higher water levels are reported at Lake Allom during this period, along with lower fire activity in the surrounding area (Donders et al., 2006), indicating that effective precipitation was higher than during the mid-Holocene.

**Summary and conclusions:**

Quantitative reconstructions of climate in the southern hemisphere are rare and yet of high importance to further our understanding of climate change and associated biological responses. This study highlights the potential of using branched GDGT distributions as a proxy for the quantitative reconstruction of trends and amplitudes of past temperature variability from lacustrine sediment archives. The apparent accuracy of the branched GDGT temperature estimates at Lake McKenzie may be at least partially due to the predominantly allochthonous origin of branched GDGTs observed in the sediments of this lake. In many lake systems, the branched GDGTs observed in sediments are likely to derive from both allochthonous and autochthonous sources (eg Blaga et al., 2009; Pearson et al., 2011; Sun et al., 2011; Tierney and Russell, 2009), making these more complex systems to infer temperatures from branched GDGT relative to Lake McKenzie.

The Lake McKenzie MAAT record presented in this study contributes to the relatively sparse array of quantitative information about temperature variability during the last glacial period on the Australian continent. The location, length, and apparent quantitative nature of the Lake McKenzie terrestrial MAAT reconstruction makes it well positioned for future paleoclimate model/data comparison studies that compare terrestrial and marine climate records to obtain new insight on the difference in response of the terrestrial climate relative to global climatic changes. This may be instrumental for better constraining future projections of climate change on the Australian continent.

**Acknowledgments:**

We would like to thank: Sarah Hembrow, Linda Barry and Kerry Wilsher for their assistance with field work at Lake McKenzie. Additionally we would like to give special thanks to Colin Lawton from the Queensland Parks and Wildlife Service for collecting and sending soil samples from the drainage basin of Lake McKenzie. Atun Zawadski, Jack Goralewski and Daniela Fierro are acknowledged for their work on the $^{210}$Pb dating and Fiona Bertuch and Alan Williams are thanked for their assistance with the AMS $^{14}$C dating. We additionally would like to thank Prof Lorenz Schwark for critical discussions about this research project

Martijn Woltering and Kliti Grice were supported by an ARC QEII Discovery grant awarded to KG. Funding for the LC-MS Orbitrap facility at Curtin University was supplied by an ARC LIEFP grant, the WA-OIGC and the John de Laeter Centre for Isotope research.

**References cited:**

Abram, N.J., McGregor, H.V., Gagan, M.K., Hantoro, W.S., Suwargadi, B.W., 2009. Oscillations in the southern extent of the Indo-Pacific Warm Pool during the mid-Holocene. Quaternary Science Reviews 28, 2794-2803.

Appleby, P.G., Oldfield, F., 1978. The calculation of lead-210 dates assuming a constant rate of supply of unsupported 210Pb to the sediment. CATENA 5, 1-8.

Appleby, P.G., Oldfield, F., 1992. Application of $^{210}$Pb to sediment studies, in: Ivonavich, M., Harmon, R.S. (Eds.), Uranium-series disequilibrium: applications to earth, marine and environmental science. Oxford University Press, Oxford, pp. 731-778.

Appleby, P.G., 2001. Chronostratigraphic techniques in recent sediments, in: Last, W.M., Smol, J.P. (Eds.), Tracking environmental change using lake sediments, Volume 1: Basin analysis, coring and chronological techniques. Kluwer Academic Publishers, Dordrecht, pp. 171-203

Armand, L.K., Leventer, A., 2010. Palaeo sea ice distribution and reconstruction derived from the geological record. Sea Ice, 469-530.

Australian Bureau of Meteorology (BOM) 2013, Australian Government 21/12/2013, http://www.bom.gov.au/.

Barrell, D.J.A., Almond, P.C., Vandergoes, M.J., Lowe, D.J., Newnham, R.M., 2013. A composite pollen-based stratotype for inter-regional evaluation of climatic events in New Zealand over the past 30,000 years (NZ-INTIMATE project). Quaternary Science Reviews 74, 4-20.

Barrows, T.T., Juggins, S., 2005. Sea-surface temperatures around the Australian margin and Indian ocean during the last glacial maximum. Quaternary Science Reviews 24, 1017-1047.

Barrows, T.T., Juggins, S., De Deckker, P., Calvo, E., Pelejero, C., 2007. Long-term sea surface temperature and climate change in the Australian-New Zealand region. Paleoceanography 22, PA2215.

627 Barrows, T.T., Stone, J.O., Fifield, L.K., Cresswell, R.G., 2001. Late Pleistocene Glaciation of the
628 Kosciuszko Massif, Snowy Mountains, Australia. Quaternary Research 55, 179-189.
629 Bechtel, A., Smittenberg, R.H., Bernasconi, S.M., Schubert, C.J., 2010. Distribution of branched and
630 isoprenoid tetraether lipids in an oligotrophic and a eutrophic Swiss lake: Insights into sources
631 and GDGT-based proxies. Organic Geochemistry 41, 822-832.
632 Blaga, C.I., Reichart, G.J., Heiri, O., Sinninghe Damsté, J.S., 2009. Tetraether membrane lipid
633 distributions in water-column particulate matter and sediments: a study of 47 European lakes
634 along a north-south transect. Journal of Paleolimnology 41, 523-540.
635 Blunier, T., Brook, E.J., 2001. Timing of millennial-scale climate change in Antarctica and Greenland
636 during the last glacial period. science 291, 109-112.
637 Bostock, H.C., Opdyke, B.N., Gagan, M.K., Kiss, A.E., Fifield, L.K., 2006. Glacial/interglacial
638 changes in the East Australian current. Climate dynamics 26, 645-659.
639 Bowler, J.M., 1976. Aridity in Australia: Age, origins and expression in aeolian landforms and
640 sediments. Earth-Science Reviews 12, 279-310.
641 Bowler, J.M., Gillespie, R., Johnston, H., Boljkovac, K., 2012. Wind v water: glacial maximum
642 records from the Willandra Lakes. Terra Australis 34, 271-296.
643 Bowling, L.C., 1988. Optical properties, nutrients and phytoplankton of freshwater coastal dune lakes
644 in south-east Queensland. Austalian Journal fo Freshwater Research. 39, 805-815.
645 Bronk Ramsey, C., 2009. Bayesian analysis of radiocarbon dates. Radiocarbon 51, 337-360.
646 Calvo, E., Pelejero, C., De Deckker, P., Logan, G.A., 2007. Antarctic deglacial pattern in a 30 kyr
647 record of sea surface temperature offshore South Australia. Geophysical Research Letters 34,
648 1-6.
649 Castaneda, I.S., Schouten, S., 2011. A review of molecular organic proxies for examining modern and
650 ancient lacustrine environments. Quaternary Science Reviews 30, 2851-2891.
651 Clark, P.U., Dyke, A.S., Shakun, J.D., Carlson, A.E., Clark, J., Wohlfarth, B., Mitrovica, J.X.,
652 Hostetler, S.W., McCabe, A.M., 2009. The last glacial maximum. science 325, 710-714.
653 D'Costa, D.M., Edney, P., Kershaw, A.P., Deckker, P.D., 1989. Late Quaternary Palaeoecology of
654 Tower Hill, Victoria, Australia. Journal of Biogeography 16, 461-482.
655 Das, S.K., Bendle, J., Routh, J., 2012. Evaluating branched tetraether lipid-based palaeotemperature
656 proxies in an urban, hyper-eutrophic polluted lake in South Africa. Organic Geochemistry 53,
657 45-51.
658 De Deckker, P., Moros, M., Perner, K., Jansen, E., 2012. Influence of the tropics and southern
659 westerlies on glacial interhemispheric asymmetry. Nature Geoscience 5, 266-269.
660 Denton, G.H., Lowell, T.V., Heusser, C.J., Moreno, P.I., Andersen, B.G., Heusser, L.E., Schlüchter,
661 C., Marchant, D.R., 1999. Interhemispheric Linkage of Paleoclimate during the Last
662 Glaciation. Geografiska Annaler. Series A, Physical Geography 81, 107-153.
663 Donders, T.H., Wagner, F., Visscher, H., 2006. Late Pleistocene and Holocene subtropical vegetation
664 dynamics recorded in perched lake deposits on Fraser Island, Queensland, Australia.
665 Palaeogeography Palaeoclimatology Palaeoecology 241, 417-439.
666 EPICA Members,, 2006. One-to-one coupling of glacial climate variability in Greenland and
667 Antarctica. Nature 444, 195-198.
668 Fawcett, P.J., Werne, J.P., Anderson, R.S., Heikoop, J.M., Brown, E.T., Berke, M.A., Smith, S.J.,
669 Goff, F., Donohoo-Hurley, L., Cisneros-Dozal, L.M., Schouten, S., Damste, J.S.S., Huang,
670 Y.S., Toney, J., Fessenden, J., WoldeGabriel, G., Atudorei, V., Geissman, J.W., Allen, C.D.,
671 2011. Extended megadroughts in the southwestern United States during Pleistocene
672 interglacials. Nature 470, 518-521.
673 Gagan, M.K., Ayliffe, L.K., Hopley, D., Cali, J.A., Mortimer, G.E., Chappell, J., McCulloch, M.T.,
674 Head, M.J., 1998. Temperature and Surface-Ocean Water Balance of the Mid-Holocene
675 Tropical Western Pacific. science 279, 1014-1018.
676 Gagan, M.K., Hendy, E.J., Haberle, S.G., Hantoro, W.S., 2004. Post-glacial evolution of the Indo-
677 Pacific Warm Pool and El Niño-Southern oscillation. Quaternary International 118–119, 127-
678 143.
679 Hadwen, W.L., 2002. Effects of nutrient additions on dune lakes on Fraser Island, Australia, Faculty
680 of Environmental Sciences. Griffith University, Brisbane.

Harrison, S.P., 1993. Late Quaternary lake-level changes and climates of Australia. Quaternary Science Reviews 12, 211-231.
Hellstrom, J., McCulloch, M., Stone, J., 1998. A detailed 31,000-year record of climate and vegetation change, from the isotope geochemistry of two New Zealand speleothems. Quaternary Research 50, 167-178.
Hembrow, S., Taffs, K., Atahan, P., Parr, J., Zawadzki, A., Heijnis, H., 2014. Diatom community response to climate variability over the past 37,000 years in the sub-tropics of the Southern Hemisphere. Science of the total environent. 468-469, 774-784.
Hua, Q., Zoppi, U., Williams, A.A., Smith, A.M., 2004. Small-mass AMS radiocarbon analysis at ANTARES. Nuclear Instruments and Methods in Physics Research, Section B: Beam Interactions with Materials and Atoms 223-224, 284-292.
Kershaw, A.P., 1986. Climatic change and Aboriginal burning in north-east Australia during the last two glacial/interglacial cycles. Nature 322, 47-49.
Kershaw, A.P., Nanson, G.C., 1993. The last full glacial cycle in the australian region. Global and Planetary Change 7, 1-9.
Longmore, M.E., 1997. Quaternary palynological records from perched lake sediments, Fraser Island, Queensland, Australia: Rainforest, forest history and climatic control. Australian Journal of Botany 45, 507-526.
Longmore, M.E., Heijnis, H., 1999. Aridity in Australia: Pleistocene records of Palaeohydrological and Palaeoecological change from the perched lake sediments of Fraser Island, Queensland, Australia. Quaternary International 57-8, 35-47.
Loomis, S.E., Russell, J.M., Ladd, B., Street-Perrott, F.A., Sinninghe Damsté, J.S., 2012. Calibration and application of the branched GDGT temperature proxy on East African lake sediments. Earth and Planetary Science Letters 357–358, 277-288.
Loomis, S.E., Russell, J.M., Sinninghe Damsté, J.S., 2011. Distributions of branched GDGTs in soils and lake sediments from western Uganda: Implications for a lacustrine paleothermometer. Organic Geochemistry 42, 739-751.
McKenzie, N., Jacquier, D., Isbell, R., Brown, K., 2004. Australian soils and landscapes: an illustrated compendium. CSIRO Publishing, Collingwood, Australia.
Miller, G.H., Magee, J.W., Jull, A.J.T., 1997. Low-latitude glacial cooling in the Southern Hemisphere from amino-acid racemization in emu eggshells. Nature 385, 241-244.
Moss, P.T., Kershaw, A.P., 2000. The last glacial cycle from the humid tropics of northeastern Australia: comparison of a terrestrial and a marine record. Palaeogeography Palaeoclimatology Palaeoecology 155, 155-176.
Moss, P.T., Kershaw, A.P., 2007. A late Quaternary marine palynological record (oxygen isotope stages 1 to 7) for the humid tropics of northeastern Australia based on ODP Site 820. Palaeogeography Palaeoclimatology Palaeoecology 251, 4-22.
Niemann, H., Stadnitskaia, A., Wirth, S.B., Gilli, A., Anselmetti, F.S., Sinninghe Damsté, J.S., Schouten, S., Hopmans, E.C., Lehmann, M.F., 2012. Bacterial GDGTs in Holocene sediments and catchment soils of a high Alpine lake: application of the MBT/CBT-paleothermometer. Clim. Past 8, 889-906.
Pearson, E.J., Juggins, S., Talbot, H.M., Weckstrom, J., Rosen, P., Ryves, D.B., Roberts, S.J., Schmidt, R., 2011. A lacustrine GDGT-temperature calibration from the Scandinavian Arctic to Antarctic: Renewed potential for the application of GDGT-paleothermometry in lakes. Geochimica et Cosmochimica Acta 75, 6225-6238.
Peterse, F., Prins, M.A., Beets, C.J., Troelstra, S.R., Zheng, H., Gu, Z., Schouten, S., Damsté, J.S.S., 2011. Decoupled warming and monsoon precipitation in East Asia over the last deglaciation. Earth and Planetary Science Letters 301, 256-264.
Peterse, F., van der Meer, J., Schouten, S., Weijers, J.W.H., Fierer, N., Jackson, R.B., Kim, J.H., Sinninghe Damsté, J.S., 2012. Revised calibration of the MBT-CBT paleotemperature proxy based on branched tetraether membrane lipids in surface soils Geochimica et Cosmochimica Acta 96, 215-219.
Petherick, L., Bostock, H., Cohen, T.J., Fitzsimmons, K., Tibby, J., Fletcher, M.S., Moss, P., Reeves, J., Mooney, S., Barrows, T., 2013. Climatic records over the past 30 ka from temperate

735 Australia–a synthesis from the Oz-INTIMATE workgroup. Quaternary Science Reviews 74,
736 58-77.
737 Pickett, E.J., Harrison, S.P., Hope, G., Harle, K., Dodson, J.R., Peter Kershaw, A., Colin Prentice, I.,
738 Backhouse, J., Colhoun, E.A., D'Costa, D., Flenley, J., Grindrod, J., Haberle, S., Hassell, C.,
739 Kenyon, C., Macphail, M., Martin, H., Martin, A.H., McKenzie, M., Newsome, J.C., Penny,
740 D., Powell, J., Ian Raine, J., Southern, W., Stevenson, J., Sutra, J.-P., Thomas, I., van der
741 Kaars, S., Ward, J., 2004. Pollen-based reconstructions of biome distributions for Australia,
742 Southeast Asia and the Pacific (SEAPAC region) at 0, 6000 and 18,000 14C yr BP. Journal of
743 Biogeography 31, 1381-1444.
744 Reeves, J.M., Bostock, H.C., Ayliffe, L.K., Barrows, T.T., De Deckker, P., Devriendt, L.S., Dunbar,
745 G.B., Drysdale, R.N., Fitzsimmons, K.E., Gagan, M.K., 2013. Palaeoenvironmental change in
746 tropical Australasia over the last 30,000 years–a synthesis by the OZ-INTIMATE group.
747 Quaternary Science Reviews, 97-114.
748 Reimer, P.J., Baillie, M.G.L., Bard, E., Bayliss, A., Beck, J.W., Blackwell, P.G., Ramsey, C.B., Buck,
749 C.E., Burr, G.S., Edwards, R.L., Friedrich, M., Grootes, P.M., Guilderson, T.P., Hajdas, I.,
750 Heaton, T.J., Hogg, A.G., Hughen, K.A., Kaiser, K.F., Kromer, B., McCormac, F.G.,
751 Manning, S.W., Reimer, R.W., Richards, D.A., Southon, J.R., Talamo, S., Turney, C.S.M.,
752 van der Plicht, J., Weyhenmeye, C.E., 2009. Intcal09 and marine09 radiocarbon age
753 calibration curves, 0-50,000 years cal bp. Radiocarbon 51, 1111-1150.
754 Rueda, G., Rosell-Mele, A., Escala, M., Gyllencreutz, R., Backman, J., 2009. Comparison of
755 instrumental and GDGT-based estimates of sea surface and air temperatures from the
756 Skagerrak. Organic Geochemistry 40, 287-291.
757 Shakun, J.D., Clark, P.U., He, F., Marcott, S.A., Mix, A.C., Liu, Z., Otto-Bliesner, B., Schmittner, A.,
758 Bard, E., 2012. Global warming preceded by increasing carbon dioxide concentrations during
759 the last deglaciation. Nature 484, 49-54.
760 Sinninghe Damsté, J.S., Hopmans, E.C., Pancost, R.D., Schouten, S., Geenevasen, J.A.J., 2000.
761 Newly discovered non-isoprenoid glycerol dialkyl glycerol tetraether lipids in sediments.
762 Chemical Communications, 1683-1684.
763 Sinninghe Damsté, J.S., Ossebaar, J., Abbas, B., Schouten, S., Verschuren, D., 2009. Fluxes and
764 distribution of tetraether lipids in an equatorial African lake: Constraints on the application of
765 the TEX86 palaeothermometer and BIT index in lacustrine settings. Geochimica et
766 Cosmochimica Acta 73, 4232-4249.
767 Sinninghe Damsté, J.S., Ossebaar, J., Schouten, S., Verschuren, D., 2012. Distribution of tetraether
768 lipids in the 25-ka sedimentary record of Lake Challa: extracting reliable TEX86 and
769 MBT/CBT palaeotemperatures from an equatorial African lake. Quaternary Science Reviews
770 50, 43-54.
771 Suggate, R.P., 1990. Late pliocene and quaternary glaciations of New Zealand. Quaternary Science
772 Reviews 9, 175-197.
773 Sun, Q., Chu, G.Q., Liu, M.M., Xie, M.M., Li, S.Q., Ling, Y.A., Wang, X.H., Shi, L.M., Jia, G.D.,
774 Lu, H.Y., 2011. Distributions and temperature dependence of branched glycerol dialkyl
775 glycerol tetraethers in recent lacustrine sediments from China and Nepal. Journal of
776 Geophysical Research-Biogeosciences 116.
777 Tierney, J.E., Russell, J.M., 2009. Distributions of branched GDGTs in a tropical lake system:
778 Implications for lacustrine application of the MBT/CBT paleoproxy. Organic Geochemistry
779 40, 1032-1036.
780 Tierney, J.E., Russell, J.M., Eggermont, H., Hopmans, E.C., Verschuren, D., Sinninghe Damsté, J.S.,
781 2010. Environmental controls on branched tetraether lipid distributions in tropical East
782 African lake sediments. Geochimica et Cosmochimica Acta 74, 4902-4918.
783 Tierney, J.E., Russell, J.M., Huang, Y.S., Sinninghe Damsté, J.S., Hopmans, E.C., Cohen, A.S., 2008.
784 Northern hemisphere controls on tropical southeast African climate during the past 60,000
785 years. science 322, 252-255.
786 Tierney, J.E., Schouten, S., Pitcher, A., Hopmans, E.C., Sinninghe Damsté, J.S., 2012. Core and intact
787 polar glycerol dialkyl glycerol tetraethers (GDGTs) in Sand Pond, Warwick, Rhode Island
788 (USA): Insights into the origin of lacustrine GDGTs. Geochimica et Cosmochimica Acta 77,
789 561-581.

Troedson, A.L., Davies, P.J., 2001. Contrasting facies patterns in subtropical and temperate continental slope sediments: inferences from east Australian late Quaternary records. Marine Geology 172, 265-285.
Turney, C.S.M., Kershaw, A.P., James, S., Branch, N., Cowley, J., Fifield, L.K., Jacobsen, G., Moss, P., 2006. Geochemical changes recorded in Lynch's Crater, Northeastern Australia, over the past 50 ka. Palaeogeography, Palaeoclimatology, Palaeoecology 233, 187-203.
Tyler, J.J., Nederbragt, A.J., Jones, V.J., Thurow, J.W., 2010. Assessing past temperature and soil pH estimates from bacterial tetraether membrane lipids: Evidence from the recent lake sediments of Lochnagar, Scotland. Journal of Geophysical Research-Biogeosciences 115, G001109.
Vandergoes, M.J., Newnham, R.M., Preusser, F., Hendy, C.H., Lowell, T.V., Fitzsimons, S.J., Hogg, A.G., Kasper, H.U., Schluchter, C., 2005. Regional insolation forcing of late Quaternary climate change in the Southern Hemisphere. Nature 436, 242-245.
Webb, T., 1986. Is vegetation in equilibrium with climate? How to interpret late-Quaternary pollen data. Plant Ecology 67, 75-91.
Weijers, J.W.H., Schefuss, E., Schouten, S., Sinninghe Damsté, J.S., 2007a. Coupled thermal and hydrological evolution of tropical Africa over the last deglaciation. science 315, 1701-1704.
Weijers, J.W.H., Schouten, S., Hopmans, E.C., Geenevasen, J.A.J., David, O.R.P., Coleman, J.M., Pancost, R.D., Sinninghe Damsté, J.S., 2006. Membrane lipids of mesophilic anaerobic bacteria thriving in peats have typical archaeal traits. Environmental Microbiology 8, 648-657.
Weijers, J.W.H., Schouten, S., van den Donker, J.C., Hopmans, E.C., Sinninghe Damsté, J.S., 2007b. Environmental controls on bacterial tetraether membrane lipid distribution in soils. Geochimica et Cosmochimica Acta 71, 703-713.
Woltering, M., Johnson, T.C., Werne, J.P., Schouten, S., Sinninghe Damsté, J.S., 2011. Late Pleistocene temperature history of Southeast Africa: A TEX86 temperature record from Lake Malawi. Palaeogeography, Palaeoclimatology, Palaeoecology 303, 93-102.
Zink, K.-G., Vandergoes, M.J., Mangelsdorf, K., Dieffenbacher-Krall, A.C., Schwark, L., 2010. Application of bacterial glycerol dialkyl glycerol tetraethers (GDGTs) to develop modern and past temperature estimates from New Zealand lakes. Organic Geochemistry 41, 1060-1066.

List of figures:

Figure 1: **A**: Map showing the location of Fraser Island and Lake McKenzie. The black triangle (1) marks the locations of a previous paleoenvironmental study on Fraser Island at Lake Allom; (2) Sandy Cape Lighthouse weather station; (3) Maryborough weather station and (4) Eurong weather station. **B**: White circles mark the location of cores LM1 and LM2 within Lake McKenzie and locations of soil samples surrounding the lake (Google Earth version 6.2 software, 2012).

Figure 2: Tie-points between adjacent cores LM1 and LM2 based on organic carbon percentages. Depths from dated intervals from the LM1 core were transferred to core LM2 based on the assumption of linear sedimentation between these tie points.

Figure 3 **A**: Age model for core LM2 constructed using the P_sequence deposition program in OxCal 4.1 and the IntCal 09 calibration curve (Bronk Ramsey, 2009; Reimer et al., 2009). Three $^{14}C$ dates were tagged as outliers (OZ0411, OZN680 and OZN681). The combine function was applied to $^{210}Pb$ dates with very small depth differences. Combined pairs were dates M898 and M897, and M900 and M899. **B**: A separate age model was developed for the uppermost section for core LM2 based on the transferred $^{210}Pb$ dates from core LM1 using linear interpolation between tie-points based on the organic carbon percentage curves. Age estimates for the upper 7cm of the core were determined using linear interpolation, and an extrapolation based on the $^{210}Pb$ dated horizons.

Figure 4: Reconstructed temperatures based on different branched GDGT calibrations. The selection of calibration is shown here to have a significant effect on both absolute reconstructed temperature and the amplitude of past temperature variability. *ages were interpolated from the age model, where zero means AD 1950.

Figure 5: Graphs depicting the correlations between instrumentally measured mean air temperatures at Sandy Cape Lighthouse on Fraser Island and inferred temperatures using different soil and lacustrine calibrations for Lake McKenzie core LM2 branched GDGTs. Application of the soil calibration by Peterse et al. (2012) produces both a strong correlation between instrumental and inferred temperatures, and a regression line slope that is close to 1, suggesting that the calibration provides an accurate estimate of the amplitude of temperature variability.

Figure 6 **A**: The relative distribution of branched GDGT lipids measured in 3 soil samples collected within the Lake McKenzie drainage basin and in the top sediment of core LM2. The largely identical branched GDGT signals suggest a predominantly soil origin of the branched GDGT in the sediments of Lake McKenzie. **B**: Average values of 3 prominent branched GDGTs in lake and fjord sediments affected by *in situ* production of branched GDGTs (Tierney et al., 2010; Tyler et al., 2010; Sun et al., 2012) and the average distribution in soils of the global soil calibration (Weijers et al.,2007b) (this figure is modified from Sun et al., 2011). The branched GDGT distribution in Lake McKenzie largely follows the typical global soil GDGT distribution, and is significantly different to sediments where there is evidence of *in situ* production of branch GDGTs.

Figure 7: pH values obtained from the literature compared to reconstructed pH based on the soil and lake calibrations (Weijers et al. 2007b; Peterse et al., 2012; Sun et al., 2011). Reconstructed pH for the top 1cm of core LM2 using the soil calibrations is consistent with previous measurements of soil pH in the region (McKenzie et al.,2004) and reconstructed pH values for soil samples surround the lake and is substantially higher than the measured pH of the lake water (Hadwen, 2002).

Figure 8:A: Branched GDGT inferred MAAT plotted together with inferred pH values and measured percentages of total organic carbon (%TOC) in core LM2 from Lake McKenzie, B: cross plot of CBT/MBT ratio, C: Cross plot of MAAT and pH and D: cross plot MAAT and %TOC

Figure 9: Lake McKenzie branched GDGT based inferred record of MAAT variability during both the end of the last Glacial period (light grey) and the Holocene (dark grey). The dashed line reflects the modern day MAAT of 20.4$^{o}$C, as observed in the top 1cm of sediment from Lake McKenzie. Horizontal error bars depict the upper and lower age estimates for each sample, while the vertical error bars reflect the standard deviation around the mean temperature estimate using at least triplicate or more measurements of each sample. *ages were interpolated from the age model, where zero means AD 1950.

Figure 10: The Lake McKenzie MAAT record plotted together with two $\delta^{18}$O of *G. ruber* marine records located north (GC-12, Bostock et al., 2005) and south (GC-25, Troedson and Davies, 2001) of Fraser Island. Lines through the points represent a three point running averages. *ages were interpolated from the age model, where zero means AD 1950.

List of tables:

Table 1: Table of $^{14}C$ dates obtained from cores LM1 and LM2 from Lake McKenzie. LM1 depths have been converted to the core LM2 depth axis, based on linear interpolation between tie-points based on organic carbon percentages in both sediment cores.

Table2: Total $^{210}Pb$, Supported $^{210}Pb$, Unsupported $^{210}Pb$, and particle size results for samples taken from core LM1. Calendar age estimates using the CIC and CRS models are shown (Appleby and Oldfield, 1978; Appleby, 2001). Both the original depths measured on core LM1 and the corresponding depths on core LM2 are shown.

Table 3: Depths (not corrected for loss due to compaction), ages and inferred temperatures using different branched GDGT calibrations as measured in core LM2 from Lake McKenzie. MAAT = Mean Anual Air Temperature, MSAT = Mean Summer Air Temperature.*ages were interpolated from the age model where zero mean AD 1950

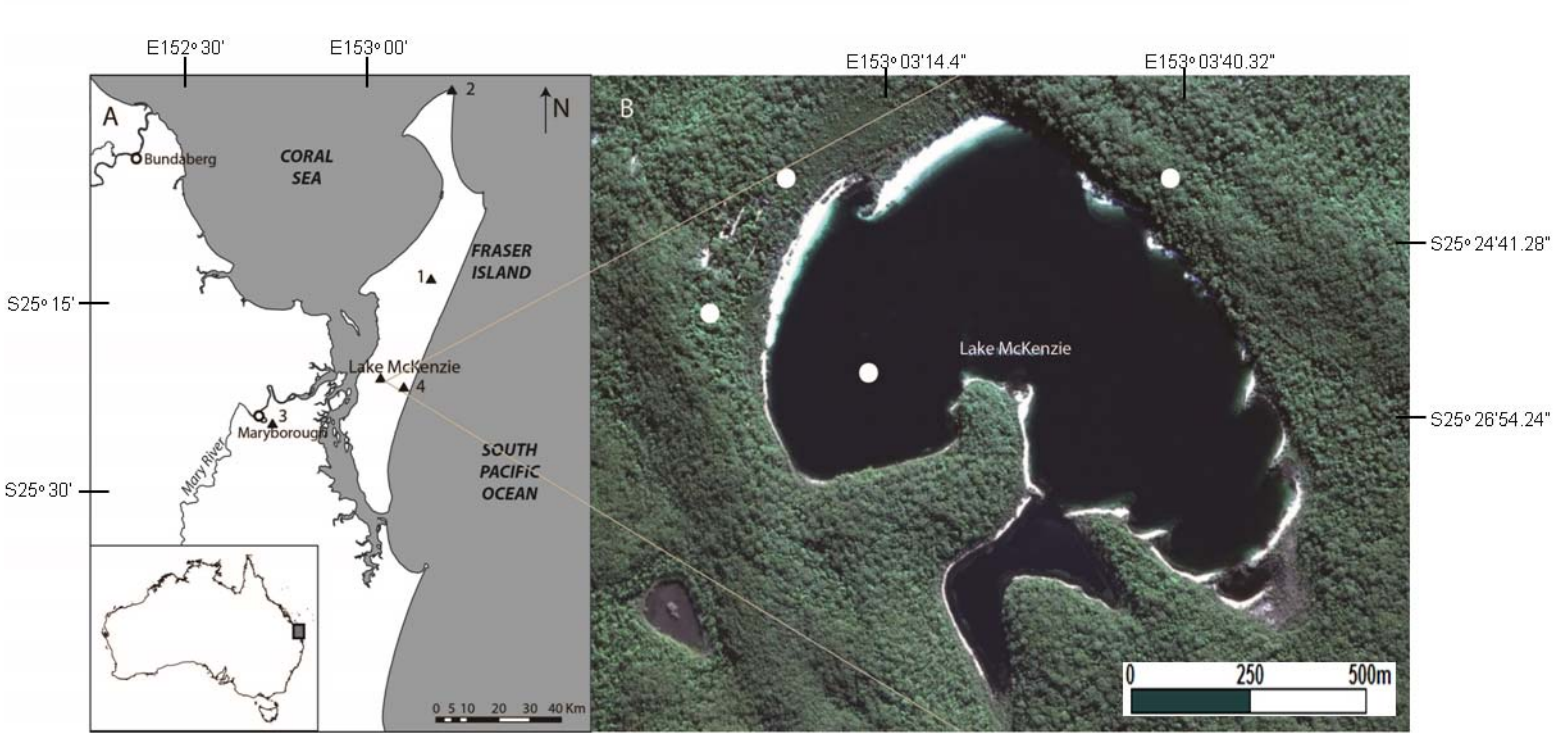
E152° 30'
E153° 00'
A
N
Bundaberg
CORAL SEA
FRASER ISLAND
1
2
S25° 15'
Lake McKenzie
4
3
Maryborough
Mary River
S25° 30'
SOUTH PACIFIC OCEAN
0 5 10 20 30 40 Km
B
E153° 03'14.4"
E153° 03'40.32"
S25° 24'41.28"
S25° 26'54.24"
Lake McKenzie
0 250 500m

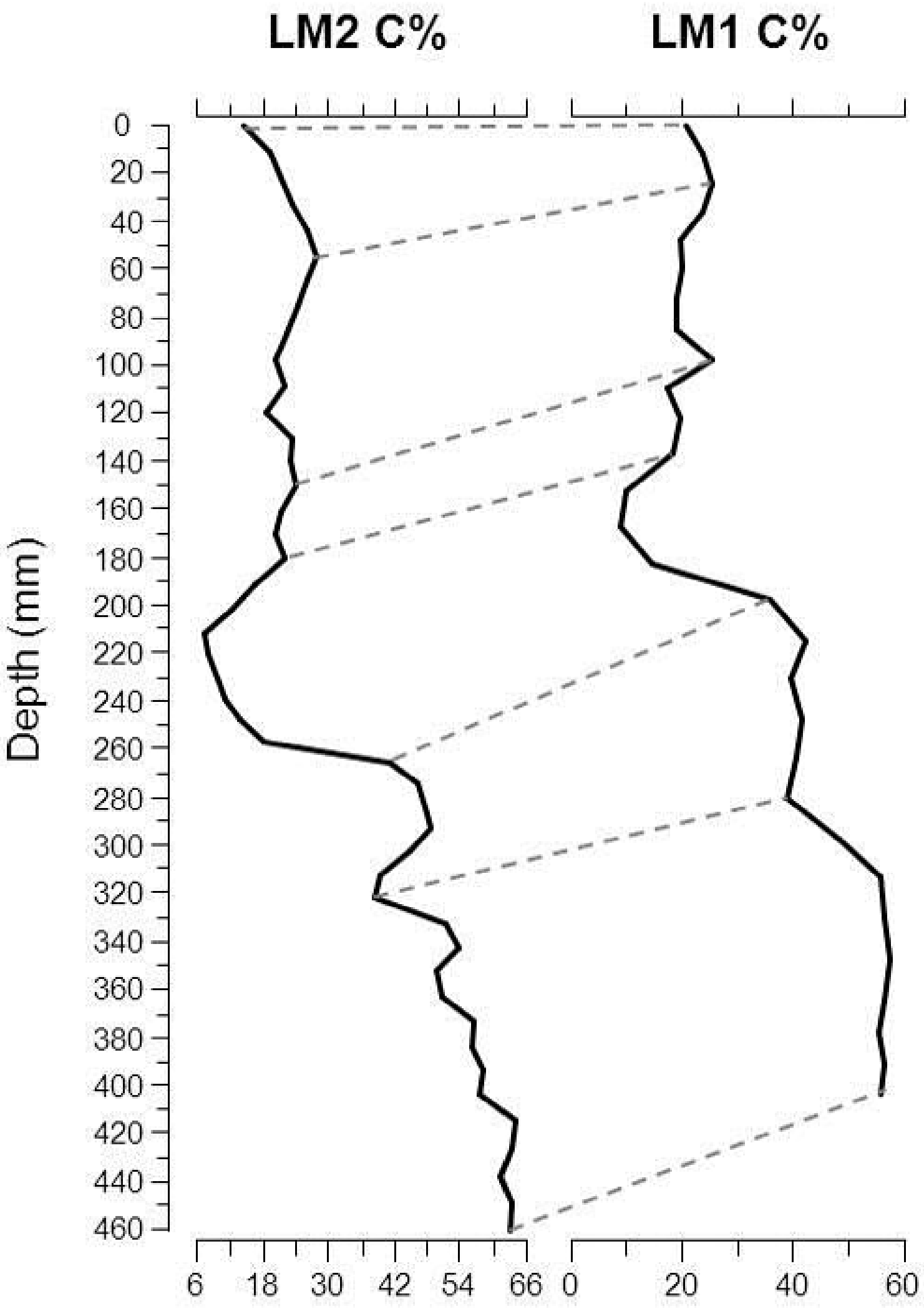
LM2 C%
LM1 C%
Depth (mm)
0
20
40
60
80
100
120
140
160
180
200
220
240
260
280
300
320
340
360
380
400
420
440
460
6
18
30
42
54
66
0
20
40
60

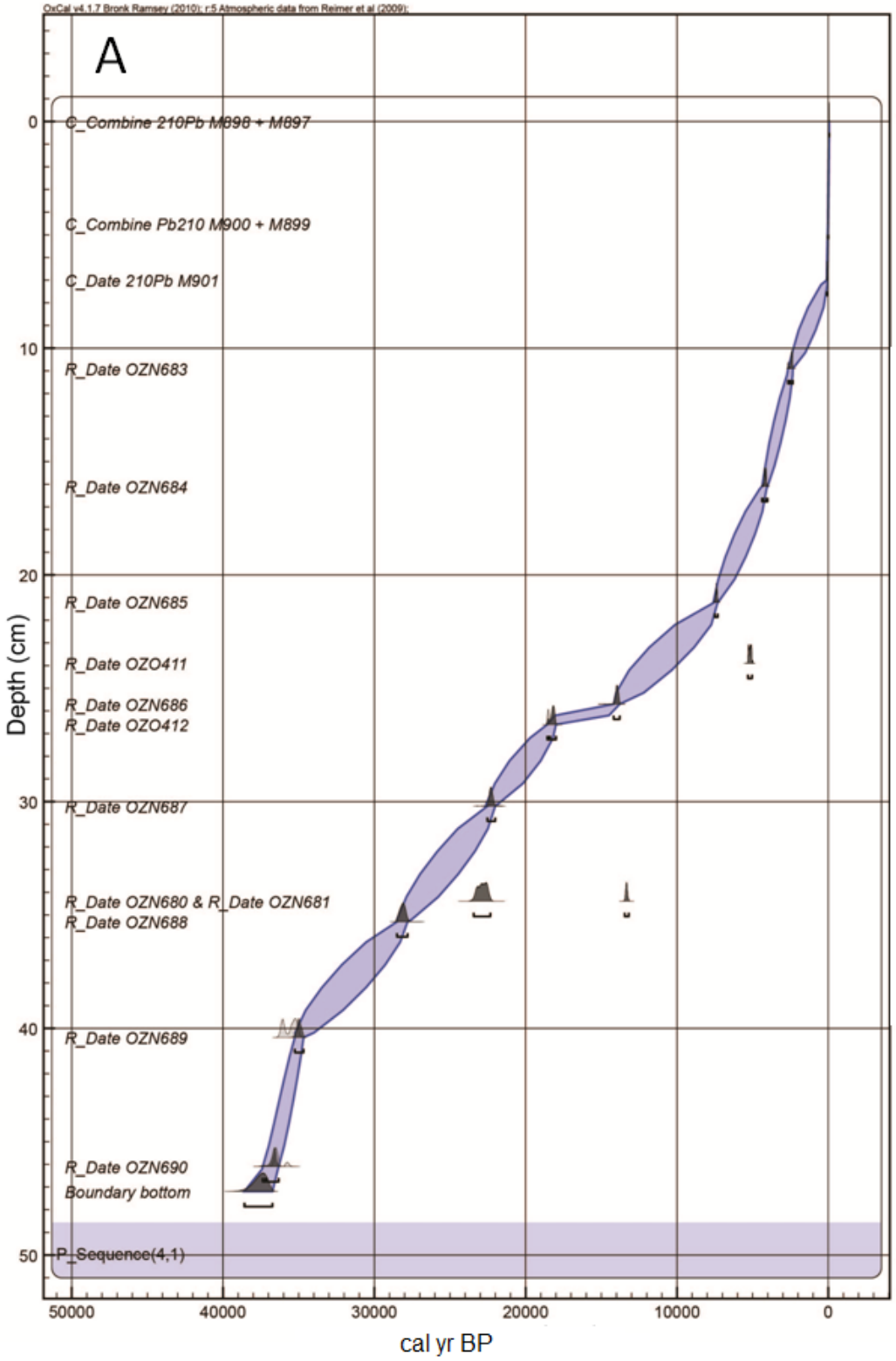
OxCal v4.1.7 Bronk Ramsey (2010); r:5 Atmospheric data from Reimer et al (2009);
A
C_Combine 210Pb M898 + M897
C_Combine Pb210 M900 + M899
C_Date 210Pb M901
R_Date OZN683
R_Date OZN684
R_Date OZN685
R_Date OZO411
R_Date OZN686
R_Date OZO412
R_Date OZN687
R_Date OZN680 & R_Date OZN681
R_Date OZN688
R_Date OZN689
R_Date OZN690
Boundary bottom
P_Sequence(4,1)
Depth (cm)
0
10
20
30
40
50
50000
40000
30000
20000
10000
0
cal yr BP

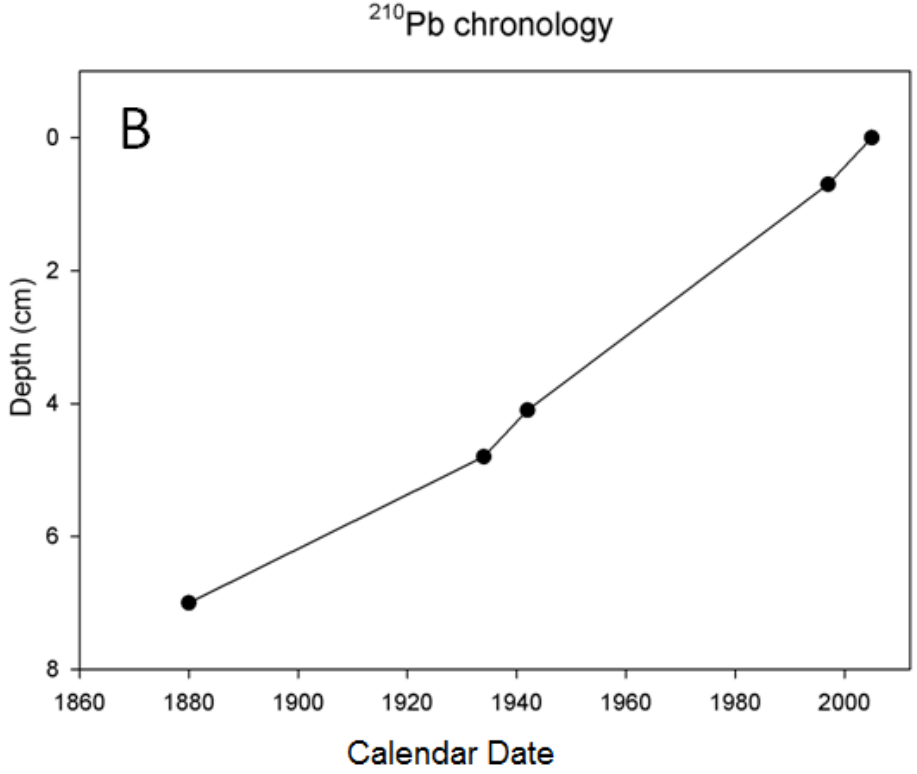
$^{210}$Pb chronology
B
Depth (cm)
0
2
4
6
8
1860
1880
1900
1920
1940
1960
1980
2000
Calendar Date

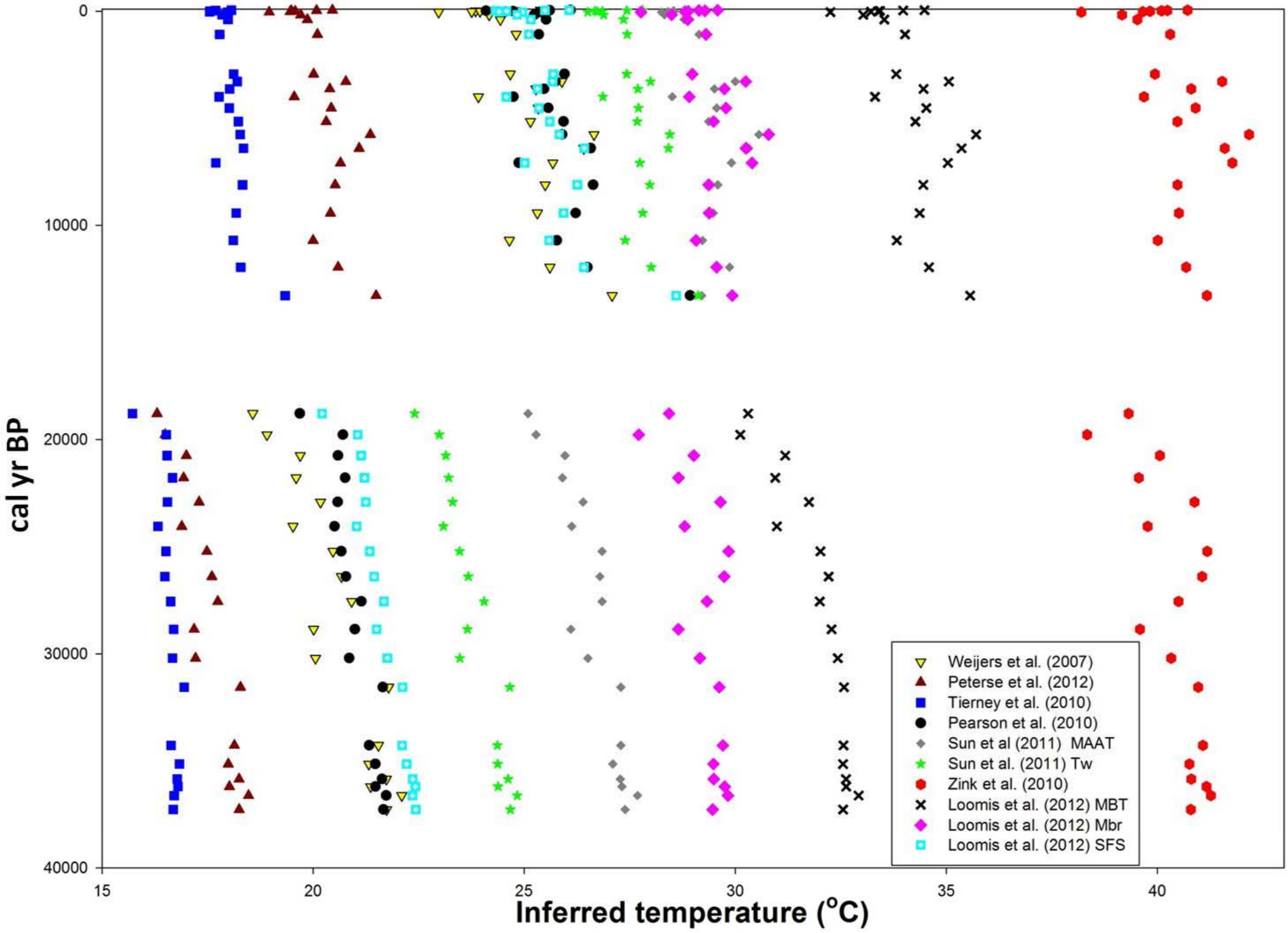
0
10000
20000
30000
40000
cal yr BP
15
20
25
30
35
40
Inferred temperature (°C)
Weijers et al. (2007)
Peterse et al. (2012)
Tierney et al. (2010)
Pearson et al. (2010)
Sun et al (2011) MAAT
Sun et al. (2011) Tw
Zink et al. (2010)
Loomis et al. (2012) MBT
Loomis et al. (2012) Mbr
Loomis et al. (2012) SFS

## Weijers et al. (2007)

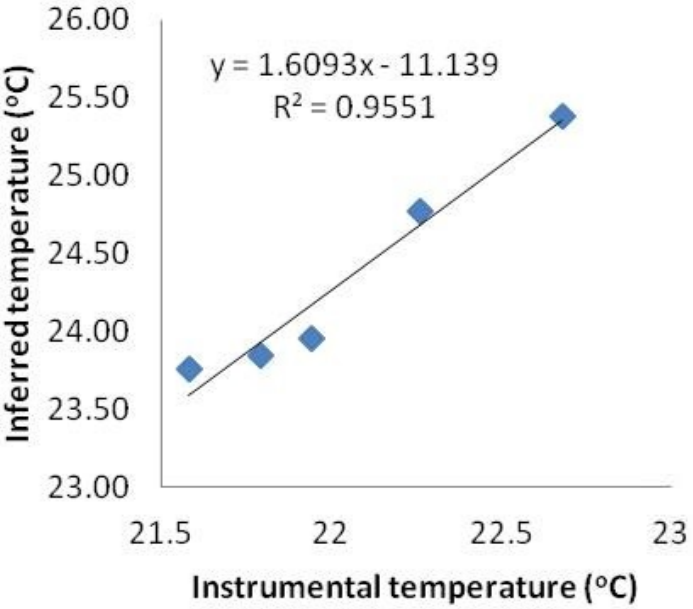


## Peterse et al. (2012)

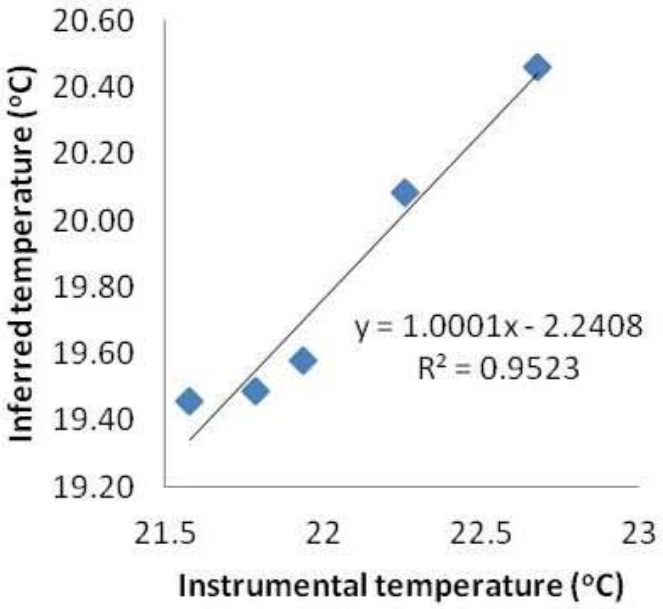


## Loomis et al. (2013) SFS

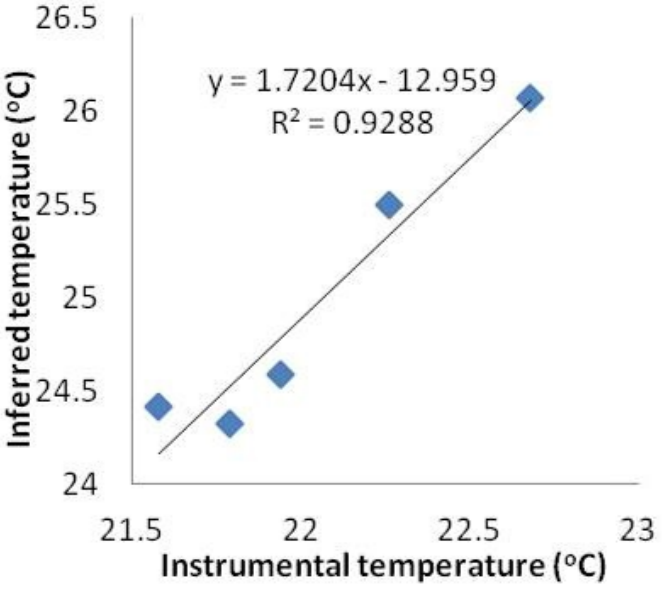


## Loomis et al. 2013 MBT

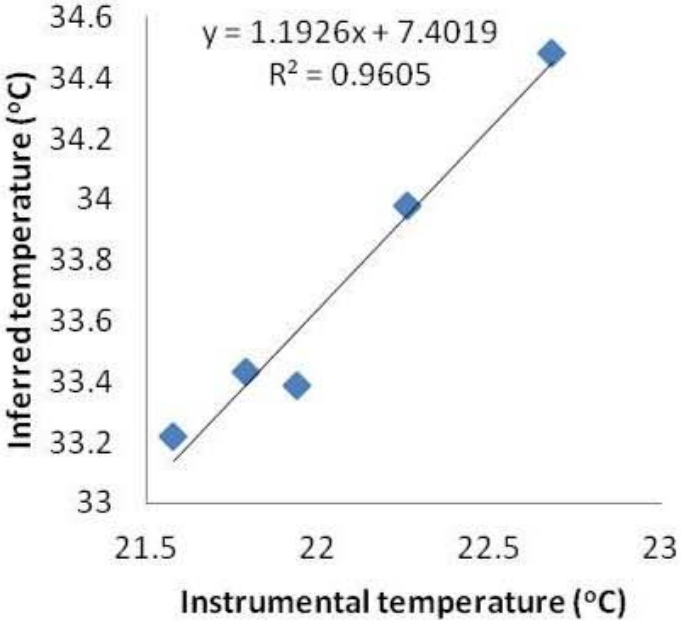


## Sun et al. (2012) MAAT

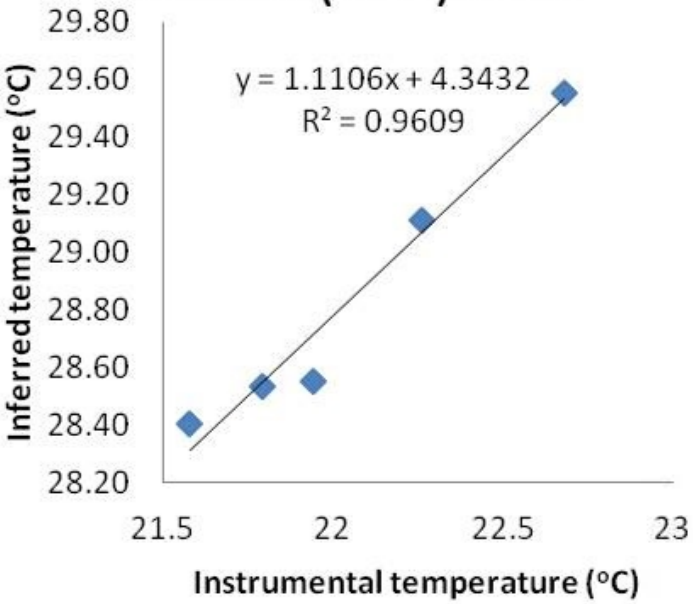


## Sun et al. (2012) Tw

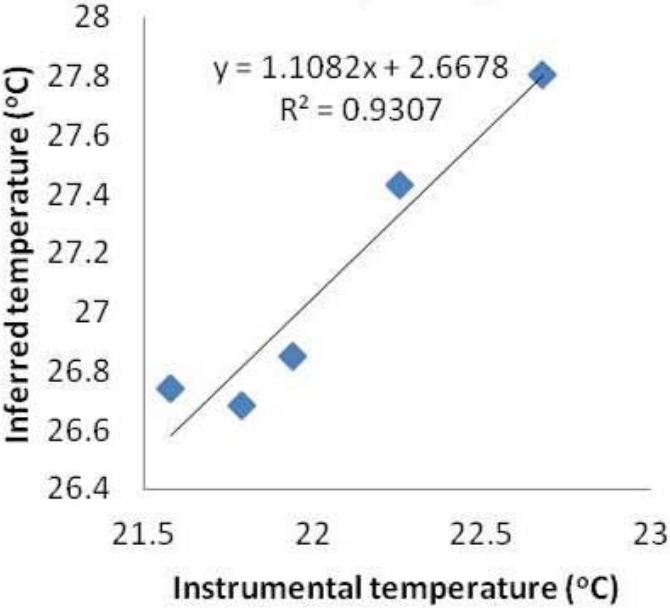

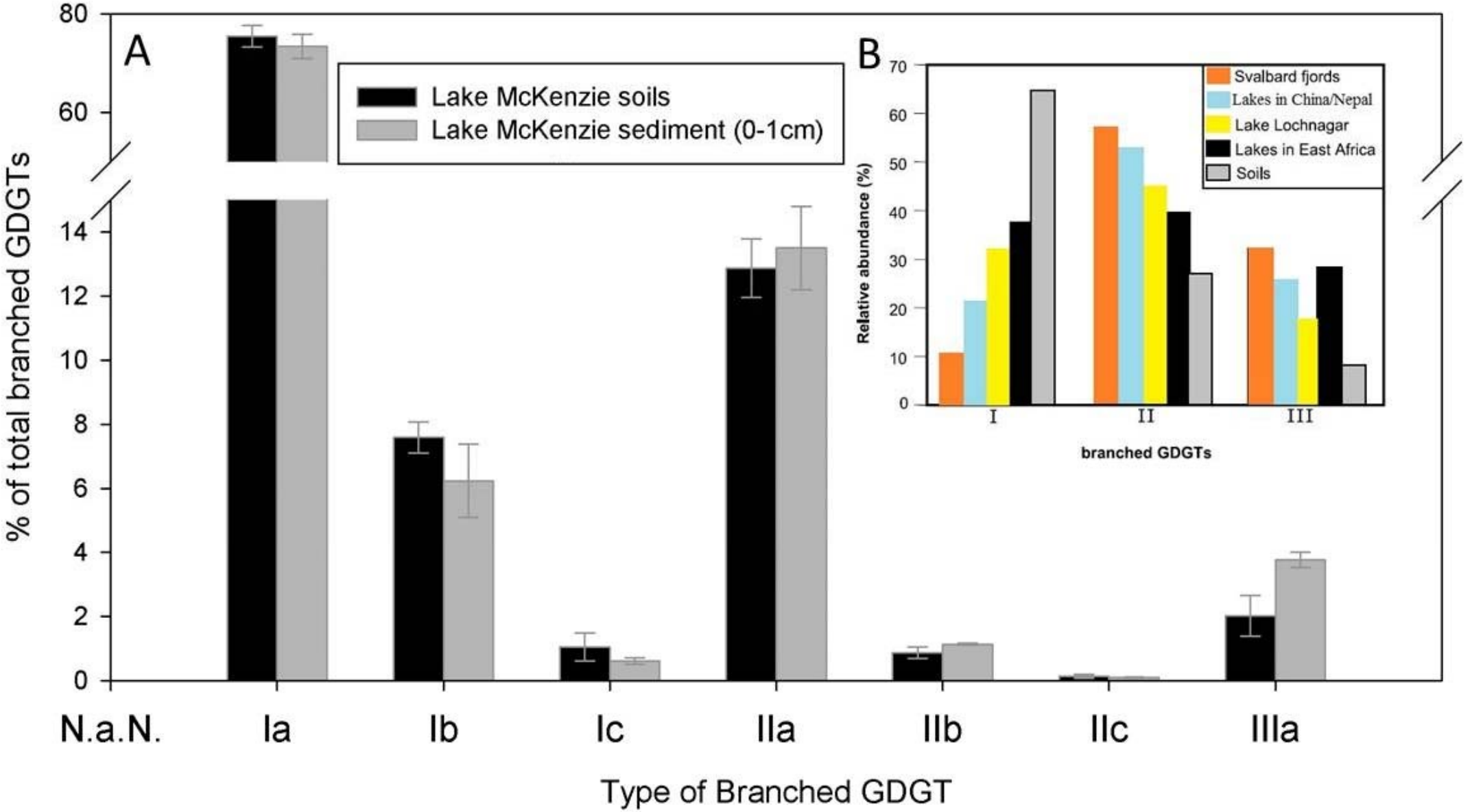
A
B
Lake McKenzie soils
Lake McKenzie sediment (0-1cm)
% of total branched GDGTs
Type of Branched GDGT
N.a.N.
Ia
Ib
Ic
IIa
IIb
IIc
IIIa
Svalbard fjords
Lakes in China/Nepal
Lake Lochnagar
Lakes in East Africa
Soils
Relative abundance (%)
branched GDGTs
I
II
III

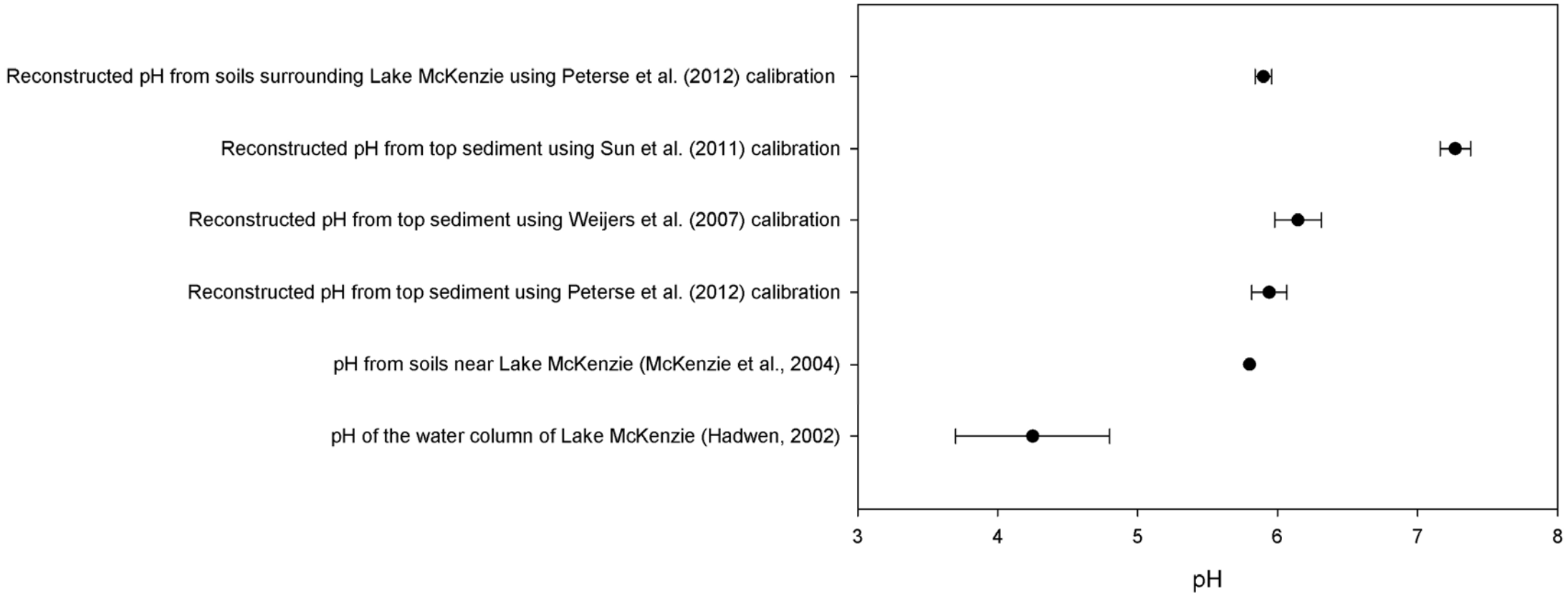
Reconstructed pH from soils surrounding Lake McKenzie using Peterse et al. (2012) calibration
Reconstructed pH from top sediment using Sun et al. (2011) calibration
Reconstructed pH from top sediment using Weijers et al. (2007) calibration
Reconstructed pH from top sediment using Peterse et al. (2012) calibration
pH from soils near Lake McKenzie (McKenzie et al., 2004)
pH of the water column of Lake McKenzie (Hadwen, 2002)
3
4
5
6
7
8
pH

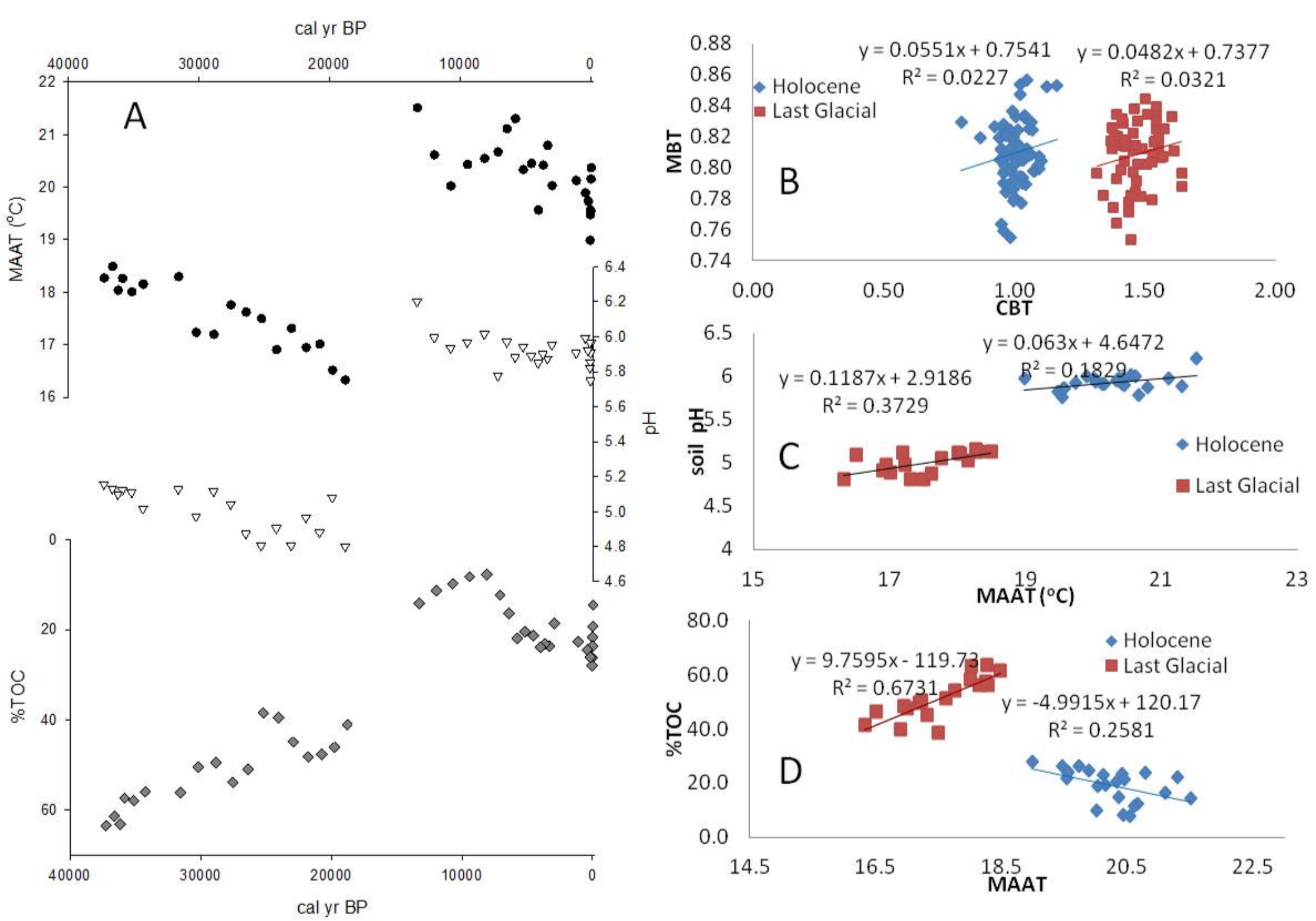
cal yr BP
40000
30000
20000
10000
0
A
MAAT (°C)
22
21
20
19
18
17
16
pH
6.4
6.2
6.0
5.8
5.6
5.4
5.2
5.0
4.8
4.6
%TOC
0
20
40
60
cal yr BP
MBT
0.88
0.86
0.84
0.82
0.80
0.78
0.76
0.74
y = 0.0551x + 0.7541
R² = 0.0227
y = 0.0482x + 0.7377
R² = 0.0321
Holocene
Last Glacial
B
0.00
0.50
1.00
1.50
2.00
CBT
soil pH
6.5
6
5.5
5
4.5
4
y = 0.063x + 4.6472
R² = 0.1829
y = 0.1187x + 2.9186
R² = 0.3729
C
Holocene
Last Glacial
15
17
19
21
23
MAAT (°C)
%TOC
80.0
60.0
40.0
20.0
0.0
y = 9.7595x - 119.73
R² = 0.6731
y = -4.9915x + 120.17
R² = 0.2581
Holocene
Last Glacial
D
14.5
16.5
18.5
20.5
22.5
MAAT

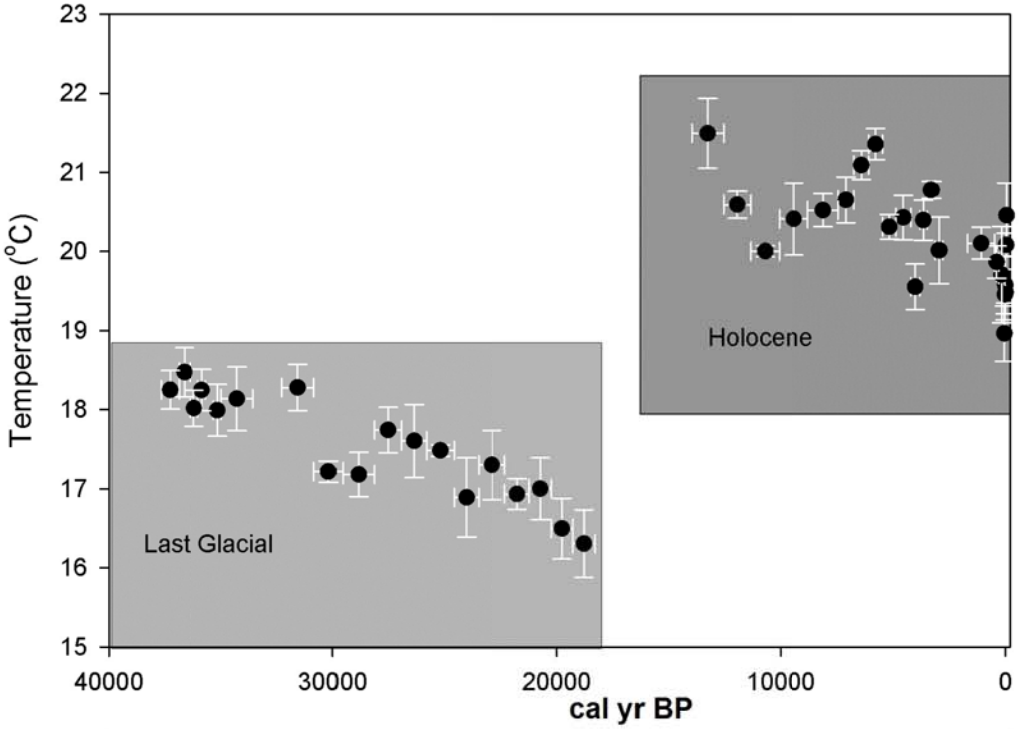
Temperature (°C)
23
22
21
20
19
18
17
16
15
Holocene
Last Glacial
40000
30000
20000
10000
0
cal yr BP

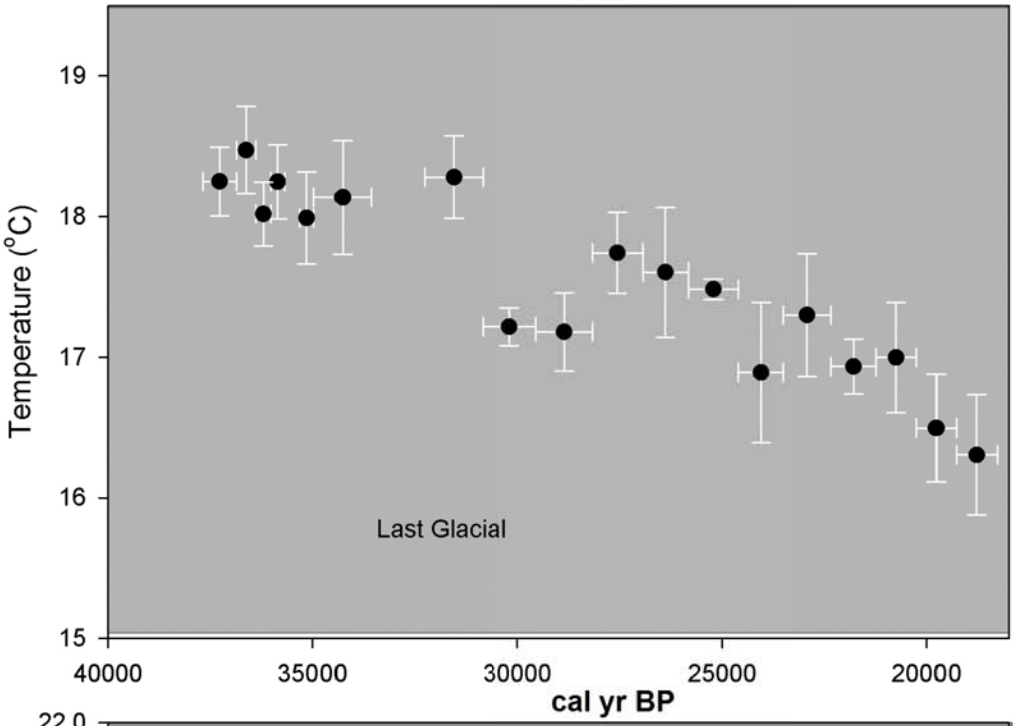
Temperature (°C)
19
18
17
16
15
Last Glacial
40000
35000
30000
25000
20000
cal yr BP

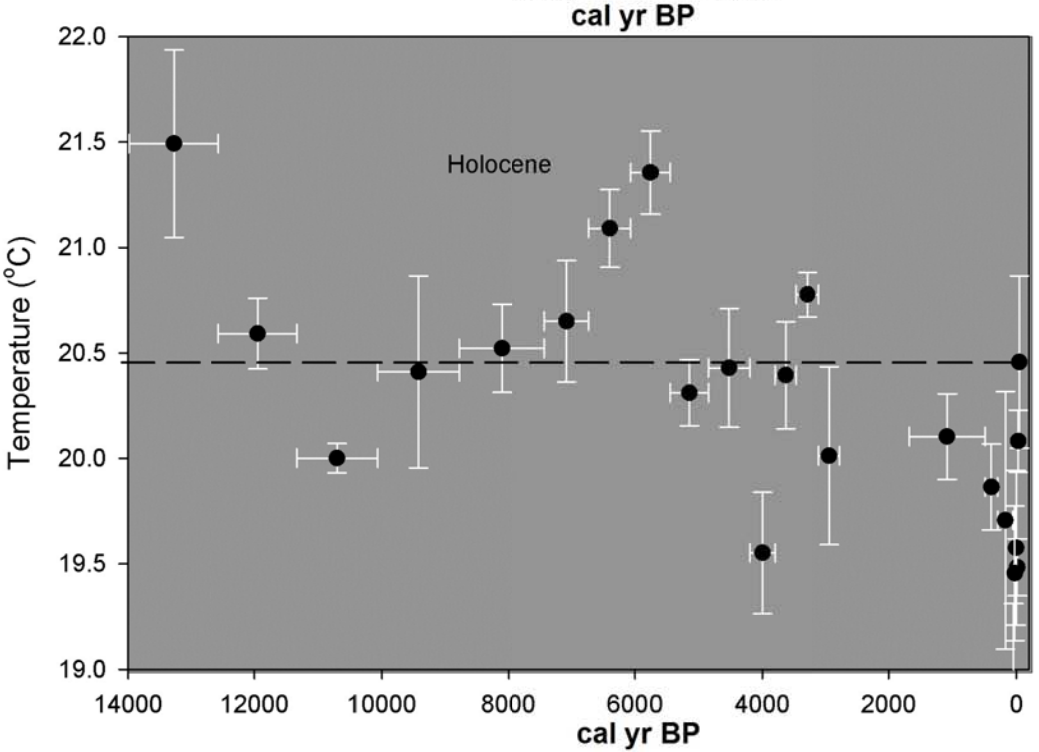
Temperature (°C)
22.0
21.5
21.0
20.5
20.0
19.5
19.0
Holocene
14000
12000
10000
8000
6000
4000
2000
0
cal yr BP

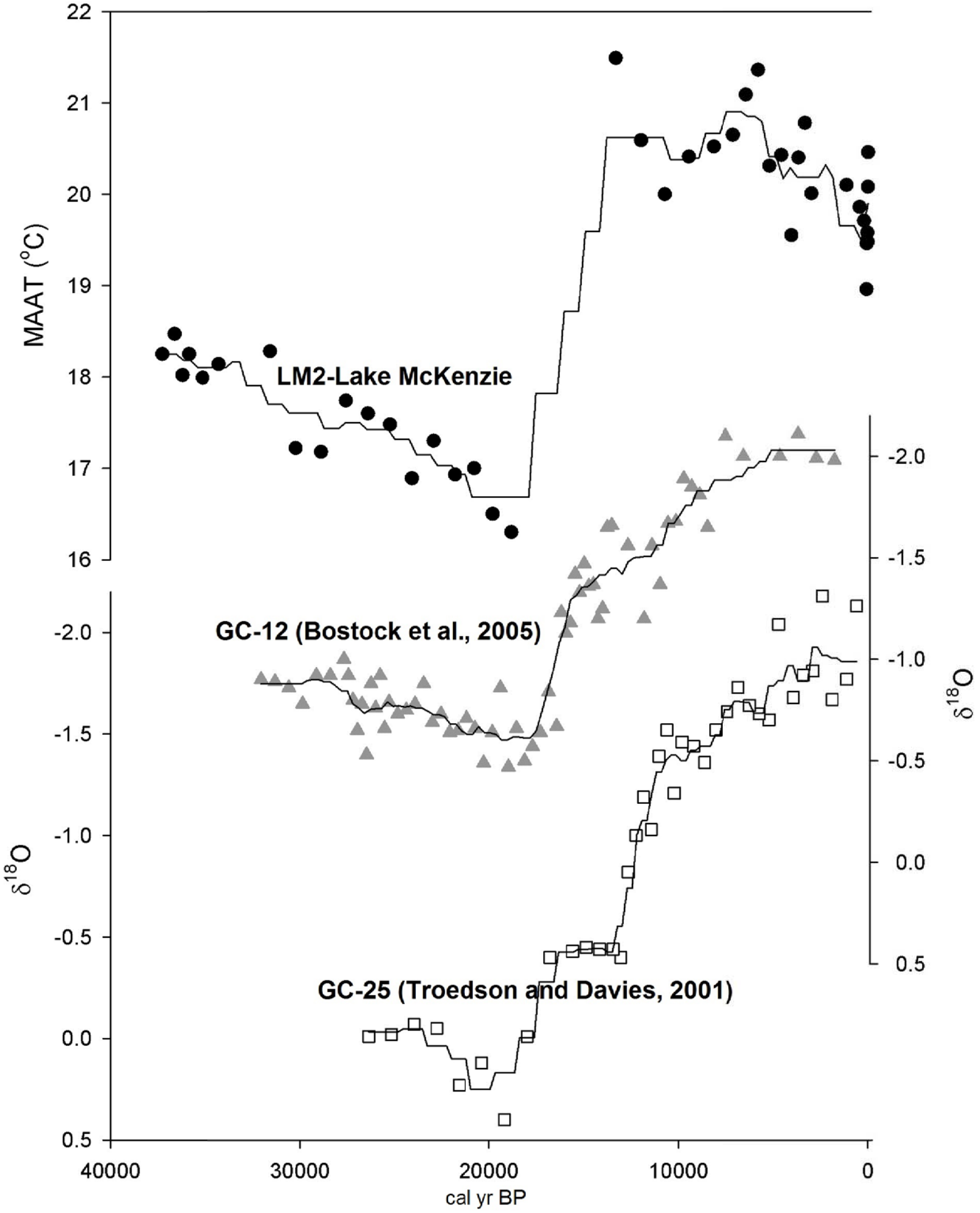
MAAT (°C)
LM2-Lake McKenzie
GC-12 (Bostock et al., 2005)
GC-25 (Troedson and Davies, 2001)
δ18O
δ18O
cal yr BP
22
21
20
19
18
17
16
-2.0
-1.5
-1.0
-0.5
0.0
0.5
40000
30000
20000
10000
0

| Lab code | Loss corrected depth (cm) | core | Composition | $^{14}$C ka BP | Error (1σ) | Calibrated age-range (cal yr BP; 2σ) |
|---|---|---|---|---|---|---|
| OZN683 | 11.9 | LM2 | Pollen | 2,395 | ± 35 | 2,183 - 2,654 |
| OZN684 | 17.1 | LM2 | Pollen | 3,785 | ± 35 | 3,931 - 4,230 |
| OZN685 | 22.1 | LM2 | Pollen | 6,485 | ± 50 | 7,260 - 7,431 |
| OZO411 | 24.8 | LM2 | Pollen | 4,515 | ± 40 | 5,309 - 5,044 |
| OZN686 | 26.6 | LM2 | Pollen | 12,110 | ± 70 | 13,786 - 14,148 |
| OZO412 | 27.5 | LM2 | Pollen | 15,100 | ± 70 | 18,589 - 18,026 |
| OZN687 | 31.2 | LM2 | Pollen | 18,670 | ± 100 | 21,872 - 22,545 |
| OZN680 | 34.4 | LM1 | Pollen | 19,150 | ± 210 | 22,330 - 23,428 |
| OZN681 | 34.4 | LM1 | Wood | 13,188 | ± 60 | 13,188 - 13,457 |
| OZN688 | 36.3 | LM2 | Pollen | 23,270 | ± 120 | 27,785 - 28,499 |
| OZN689 | 41.5 | LM2 | Pollen | 30,940 | ± 190 | 34,924 - 36,280 |
| OZN690 | 47.2 | LM2 | Pollen | 31,870 | ± 180 | 35,575 - 36,783 |

| ANSTO ID | Depth Interval measured on core LM1 (cm) | Corresponding depth interval on core LM2 (cm) | Total $^{210}$Pb (Bq/kg) | Supported $^{210}$Pb (Bq/kg) | Unsupported $^{210}$Pb* (Bq/kg) | Particle size ≤62.5 µm (%) | Calculated CIC age (years) | Calculated CRS age (years) |
|---|---|---|---|---|---|---|---|---|
| M897 | 0.00-0.25 | 0.0-0.7 | 614.4 ± 12 | 14.1 ± 2 | 601.2 ± 12 | 74.0 | 5 ± 5 | 5 ± 2 |
| M898 | 0.25-0.50 | 0.7-1.4 | 490.8 ± 24 | 17.5 ± 2 | 483.7 ± 24 | 74.0 | 15 ± 5 | 13 ± 4 |
| M899 | 1.50-1.75 | 4.1-4.8 | 168.3 ± 6 | 18.7 ± 2 | 149.9 ± 6 | 90.0 | 65 ± 7 | 64 ± 8 |
| M900 | 1.75-2.00 | 4.8-5.5 | 97.9 ± 4 | 14.7 ± 2 | 85.0 ± 5 | 77.6 | 75 ± 8 | 76 ± 9 |
| M901 | 3.00-3.50 | 7.0-7.8 | 31.0 ± 1 | 19.6 ± 2 | 11.5 ± 2 | 83.9 | 131 ± 14 | 130 ± 11 |
| M902 | 4.50-4.75 | 9.4-9.8 | 37.6 ± 1 | 27.0 ± 3 | 10.6 ± 3 | 78.9 | - | - |
| M903 | 4.75-5.00 | 9.8-10.2 | 75.6 ± 4 | 63.1 ± 6 | 12.8 ± 7 | 79.9 | - | - |
| N369 | 6.00-6.25 | 11.7-12.2 | 85.9 ± 4 | 21.9 ± 3 | 66.7 ± 5 | 69.9 | - | - |
| N370 | 6.25-6.50 | 12.2-12.6 | 101.8 ± 5 | 42.3 ± 4 | 61.8 ± 6 | 72.5 | - | - |
| N371 | 7.00-7.25 | 13.4-13.8 | 33.8 ± 2 | 32.9 ± 3 | 0.9 ± 4 | 73.3 | - | - |
| N372 | 7.25-7.50 | 13.8-14.2 | 30.9 ± 2 | 32.9 ± 3 | not detected | 83.5 | - | - |
| N373 | 8.00-8.25 | 15.0-15.2 | 62.6 ± 3 | 28.2 ± 3 | 35.8 ± 4 | 81.5 | - | - |
| N374 | 8.25-8.50 | 15.2-15.5 | 62.5 ± 3 | 32.2 ± 3 | 31.5 ± 5 | 68.7 | - | - |

*decay corrected to a fixed date

| Uncorrected Depth in core (cm) | Average age cal BP | ± | MAAT(°C) Weijers et al.(2007) | ± | MAAT(°C) Peterse et al. (2012) | ± | MAAT(°C) Sun et al. (2012) | ± | Tw(°C) Sun et al. (2012) | ± | MAAT(°C) Loomis et al. (2012)SFS | ± | MAAT(°C) Loomis et al. (2012)MBR | ± |
|---|---|---|---|---|---|---|---|---|---|---|---|---|---|---|
| 0.5 | -48 | 7 | 25.4 | 0.7 | 20.5 | 0.4 | 29.6 | 0.5 | 27.8 | 0.4 | 26.1 | 0.8 | 29.6 | 0.6 |
| 1.5 | -32 | 9 | 24.8 | 0.2 | 20.1 | 0.2 | 29.1 | 0.2 | 27.4 | 0.2 | 25.5 | 0.6 | 29.1 | 0.3 |
| 2.5 | -14 | 9 | 23.9 | 0.2 | 19.5 | 0.1 | 28.5 | 0.1 | 26.7 | 0.1 | 24.3 | 0.3 | 29.3 | 0.1 |
| 3.5 | 3 | 8 | 24.0 | 0.6 | 19.6 | 0.4 | 28.6 | 0.4 | 26.9 | 0.4 | 24.6 | 0.6 | 28.9 | 0.2 |
| 4.5 | 22 | 11 | 23.8 | 0.5 | 19.5 | 0.3 | 28.4 | 0.4 | 26.7 | 0.3 | 24.4 | 0.3 | 28.8 | 0.5 |
| 5.5 | 43 | 10 | 23.0 | 0.6 | 19.0 | 0.4 | 28.3 | 1.2 | 26.5 | 0.3 | 25.0 | 0.2 | 27.8 | 0.5 |
| 6.5 | 174 | 121 | 24.2 | 1.0 | 19.7 | 0.6 | 28.3 | 0.3 | 26.9 | 0.1 | 24.8 | 0.3 | 28.5 | 0.5 |
| 7.5 | 393 | 99 | 24.4 | 0.3 | 19.9 | 0.2 | 28.8 | 0.2 | 27.4 | 0.2 | 25.2 | 0.3 | 28.9 | 0.3 |
| 8.5 | 1083 | 591 | 24.8 | 0.3 | 20.1 | 0.2 | 29.2 | 0.2 | 27.4 | 0.3 | 25.1 | 0.5 | 29.3 | 0.1 |
| 11.5 | 2939 | 163 | 24.7 | 0.7 | 20.0 | 0.4 | 29.0 | 0.5 | 27.4 | 0.4 | 25.7 | 0.4 | 29.0 | 0.6 |
| 12.5 | 3284 | 182 | 25.9 | 0.2 | 20.8 | 0.1 | 30.0 | 0.1 | 28.0 | 0.4 | 25.7 | 1.2 | 30.2 | 0.7 |
| 13.5 | 3631 | 164 | 25.3 | 0.4 | 20.4 | 0.3 | 29.5 | 0.3 | 27.7 | 0.2 | 25.3 | 0.4 | 29.7 | 0.2 |
| 14.5 | 3996 | 201 | 23.9 | 0.5 | 19.6 | 0.3 | 28.5 | 0.4 | 26.9 | 0.2 | 24.6 | 0.3 | 28.9 | 0.5 |
| 15.5 | 4523 | 326 | 25.3 | 0.5 | 20.4 | 0.3 | 29.6 | 0.4 | 27.7 | 0.2 | 25.3 | 0.3 | 29.8 | 0.6 |
| 16.5 | 5153 | 304 | 25.2 | 0.3 | 20.3 | 0.2 | 29.4 | 0.2 | 27.7 | 0.2 | 25.6 | 0.1 | 29.5 | 0.3 |
| 17.5 | 5761 | 304 | 26.7 | 0.4 | 21.4 | 0.2 | 30.6 | 0.4 | 28.5 | 0.2 | 25.8 | 0.2 | 30.8 | 0.4 |
| 18.5 | 6399 | 334 | 26.4 | 0.3 | 21.1 | 0.2 | 30.3 | 0.3 | 28.4 | 0.1 | 26.4 | 0.3 | 30.3 | 0.5 |
| 19.5 | 7083 | 351 | 25.7 | 0.5 | 20.7 | 0.3 | 29.9 | 0.4 | 27.7 | 0.2 | 25.0 | 0.3 | 30.4 | 0.5 |
| 20.5 | 8108 | 674 | 25.5 | 0.3 | 20.5 | 0.2 | 29.6 | 0.3 | 28.0 | 0.1 | 26.3 | 0.1 | 29.4 | 0.3 |
| 21.5 | 9424 | 642 | 25.3 | 0.7 | 20.4 | 0.5 | 29.5 | 0.6 | 27.8 | 0.4 | 25.9 | 0.4 | 29.4 | 0.5 |
| 22.5 | 10699 | 633 | 24.7 | 0.1 | 20.0 | 0.1 | 29.2 | 0.5 | 27.4 | 0.0 | 25.6 | 0.1 | 29.1 | 0.2 |
| 23.5 | 11949 | 618 | 25.6 | 0.3 | 20.6 | 0.2 | 29.9 | 0.4 | 28.0 | 0.2 | 26.4 | 0.2 | 29.6 | 0.2 |
| 24.5 | 13275 | 708 | 27.1 | 0.7 | 21.5 | 0.4 | 29.2 | 2.9 | 29.1 | 0.6 | 28.6 | 1.3 | 29.9 | 0.2 |
| 26.5 | 18784 | 500 | 18.6 | 0.7 | 16.3 | 0.4 | 25.1 | 0.4 | 22.4 | 0.7 | 20.2 | 0.8 | 28.4 | 0.4 |
| 27.5 | 19767 | 484 | 18.9 | 0.6 | 16.5 | 0.4 | 25.3 | 0.5 | 23.0 | 0.4 | 21.1 | 0.2 | 27.7 | 0.4 |
| 28.5 | 20740 | 489 | 19.7 | 0.6 | 17.0 | 0.4 | 26.0 | 0.5 | 23.1 | 0.3 | 21.1 | 0.1 | 29.0 | 0.7 |
| 29.5 | 21779 | 550 | 19.6 | 0.3 | 16.9 | 0.2 | 25.9 | 0.3 | 23.2 | 0.0 | 21.2 | 0.0 | 28.7 | 0.6 |
| 30.5 | 22913 | 584 | 20.2 | 0.7 | 17.3 | 0.4 | 26.4 | 0.4 | 23.3 | 0.5 | 21.2 | 0.2 | 29.6 | 0.3 |
| 31.5 | 24048 | 552 | 19.5 | 0.8 | 16.9 | 0.5 | 26.1 | 0.7 | 23.1 | 0.5 | 21.0 | 0.3 | 28.8 | 0.6 |
| 32.5 | 25215 | 616 | 20.5 | 0.1 | 17.5 | 0.1 | 26.9 | 0.3 | 23.5 | 0.0 | 21.3 | 0.0 | 29.8 | 0.3 |
| 33.5 | 26388 | 557 | 20.7 | 0.8 | 17.6 | 0.5 | 26.8 | 0.6 | 23.7 | 0.4 | 21.4 | 0.2 | 29.7 | 0.5 |
| 34.5 | 27550 | 605 | 20.9 | 0.5 | 17.7 | 0.3 | 26.9 | 0.5 | 24.1 | 0.2 | 21.7 | 0.1 | 29.3 | 0.9 |
| 35.5 | 28852 | 697 | 20.0 | 0.5 | 17.2 | 0.3 | 26.1 | 0.3 | 23.7 | 0.3 | 21.5 | 0.2 | 28.7 | 0.4 |
| 36.5 | 30198 | 649 | 20.1 | 0.2 | 17.2 | 0.1 | 26.5 | 0.5 | 23.5 | 0.2 | 21.8 | 0.3 | 29.2 | 0.4 |
| 37.5 | 31556 | 710 | 21.8 | 0.5 | 18.3 | 0.3 | 27.3 | 0.4 | 24.7 | 0.4 | 22.1 | 0.2 | 29.6 | 0.3 |
| 39.5 | 34267 | 700 | 21.6 | 0.7 | 18.1 | 0.4 | 27.3 | 0.4 | 24.4 | 0.4 | 22.1 | 0.2 | 29.7 | 0.4 |
| 40.5 | 35138 | 171 | 21.3 | 0.5 | 18.0 | 0.3 | 27.1 | 0.3 | 24.4 | 0.3 | 22.2 | 0.2 | 29.5 | 0.3 |
| 42.5 | 35843 | 169 | 21.7 | 0.4 | 18.3 | 0.3 | 27.3 | 0.4 | 24.6 | 0.3 | 22.4 | 0.2 | 29.5 | 0.3 |
| 43.5 | 36193 | 180 | 21.4 | 0.4 | 18.0 | 0.2 | 27.3 | 0.4 | 24.4 | 0.3 | 22.4 | 0.3 | 29.8 | 0.5 |
| 44.5 | 36613 | 240 | 22.1 | 0.3 | 18.5 | 0.3 | 27.7 | 0.4 | 24.8 | 0.3 | 22.4 | 0.5 | 29.8 | 0.7 |
| 45.5 | 37261 | 407 | 21.7 | 0.4 | 18.3 | 0.2 | 27.4 | 0.3 | 24.7 | 0.3 | 22.4 | 0.3 | 29.5 | 0.1 |